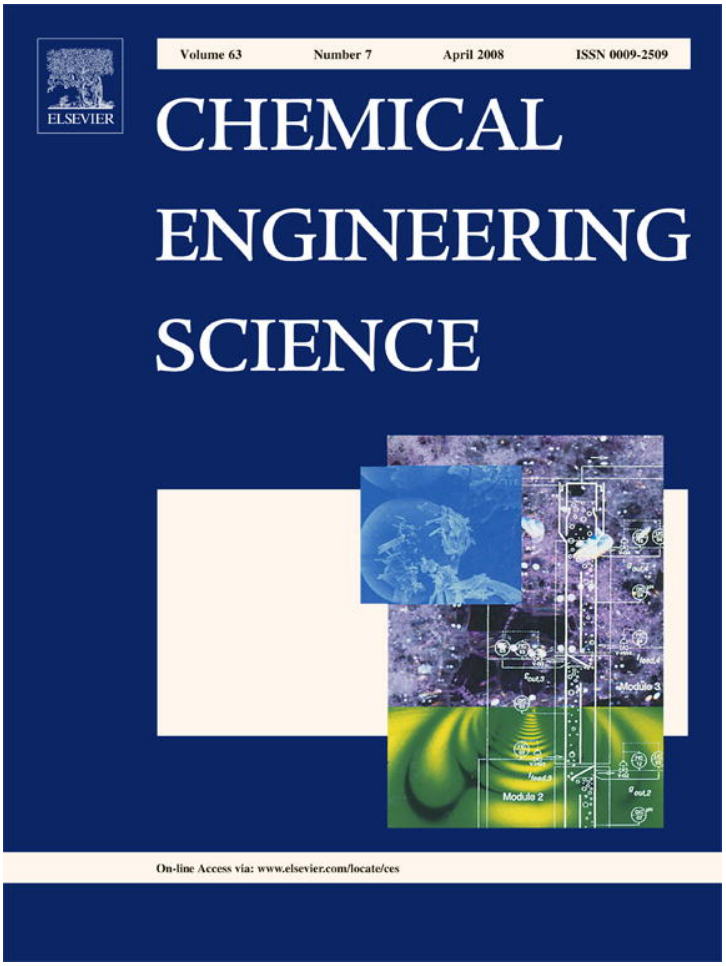

ELSEVIER

Chemical Engineering Science 63 (2008) 1800–1816

Chemical Engineering Science

www.elsevier.com/locate/ces

Model parameter estimation and feedback control of surface roughness in a sputtering process

Gangshi Hu[a], Yiming Lou[b], Panagiotis D. Christofides[a,c,*]

[a]*Department of Chemical and Biomolecular Engineering, University of California, Los Angeles, CA 90095, USA*
[b]*Advanced Projects Research, Inc., 1925 McKinley Ave. Suite B, La Verne, CA 91750, USA*
[c]*Department of Electrical Engineering, University of California, Los Angeles, CA 90095, USA*

Received 9 July 2007; received in revised form 1 December 2007; accepted 5 December 2007
Available online 14 December 2007

Abstract

This work focuses on model parameter estimation and model-based output feedback control of surface roughness in a sputtering process which involves two surface micro-processes: atom erosion and surface diffusion. This sputtering process is simulated using a kinetic Monte Carlo (kMC) simulation method and its surface height evolution can be adequately described by the stochastic Kuramoto–Sivashinsky equation (KSE), a fourth-order nonlinear stochastic partial differential equation (PDE). First, we estimate the four parameters of the stochastic KSE so that the expected surface roughness profile predicted by the stochastic KSE is close (in a least-square sense) to the profile of the kMC simulation of the same process. To perform this model parameter estimation task, we initially formulate the nonlinear stochastic KSE into a system of infinite nonlinear stochastic ordinary differential equations (ODEs). A finite-dimensional approximation of the stochastic KSE is then constructed that captures the dominant mode contribution to the state and the evolution of the state covariance of the stochastic ODE system is derived. Then, a kMC simulator is used to generate representative surface snapshots during process evolution to obtain values of the state vector of the stochastic ODE system. Subsequently, the state covariance of the stochastic ODE system that corresponds to the sputtering process is computed based on the kMC simulation results. Finally, the model parameters of the nonlinear stochastic KSE are obtained by using least-squares fitting so that the state covariance computed from the stochastic KSE process model matches that computed from kMC simulations. Subsequently, we use appropriate finite-dimensional approximations of the identified stochastic KSE model to design state and output feedback controllers, which are applied to the kMC model of the sputtering process. Extensive closed-loop system simulations demonstrate that the controllers reduce the expected surface roughness by 55% compared to the corresponding values under open-loop operation.

Keywords: Multiscale systems; Feedback control; Sputtering processes; Model reduction

1. Introduction

Thin film technology plays a crucial role in a wide range of industries such as micro-electronics, communications, optical electronics and energy. The electrical and mechanical properties of thin films strongly depend on micro-structural features such as interface width, island density and size distributions (Akiyama et al., 2002; Lee et al., 1999) and significantly affect device performance. To fabricate thin film devices with high and consistent performance, it is desirable that the operation of thin film preparation processes can be tightly controlled so that the increasingly stringent industrial requirements on the quality of such films can be satisfied. This has motivated extensive recent research on feedback control and optimization of thin film growth processes to achieve desired material micro-structure (see, for example, a recent review paper by Christofides and Armaou, 2006 and the references therein).

Sputtering processes are widely used in the thin film and semiconductor fabrication to remove materials from the surface of solids through the impact of energetic particles. In many cases sputtering is used to smooth out surface features. The surface morphology of thin films after sputter erosion strongly

* Corresponding author. Department of Chemical and Biomolecular, University of California, Los Angeles, CA 90095, USA. Tel.: +1 310 794 1015; fax: +1 310 206 4107.
E-mail addresses: gangshi@seas.ucla.edu (G. Hu), ylou@ieee.org (Y. Lou), pdc@seas.ucla.edu (P.D. Christofides).

0009-2509/$ - see front matter © 2007 Elsevier Ltd. All rights reserved.
doi:10.1016/j.ces.2007.12.008

depends on conditions such as incident ion energy, sputtered substrate temperature and material composition (Makeev et al., 2002). In a sputtering process, the surface is directly shaped by microscopic surface processes (e.g., erosion, diffusion and surface reaction), which are stochastic processes. Therefore, the stochastic nature of sputtering processes must be fully considered in the modeling and control of the surface roughness of such processes. The desire to understand and control thin film micro-structure has motivated extensive research on fundamental mathematical models describing the microscopic features of surfaces formed by surface micro-processes, which include: (1) kinetic Monte Carlo (kMC) methods (Gillespie, 1976; Fichthorn and Weinberg, 1991; Shitara et al., 1992; Reese et al., 2001) and (2) stochastic partial differential equations (PDEs) (Edwards and Wilkinson, 1982; Vvedensky et al., 1993; Cuerno et al., 1995; Lauritsen et al., 1996). Furthermore, the development of modern surface roughness measurement techniques provides the opportunity to obtain surface roughness measurements in real-time using spectroscopic ellipsometry techniques (Zapien et al., 2001), grazing-incidence small-angle X-ray scattering (GISAXS) (Renaud et al., 2003) or by combination of on-line measurement techniques for measuring gas phase compositions with off-line measurement techniques for measuring surface roughness. An implementation of the latter approach can be found in Ni et al. (2004), where it was used to measure carbon composition of thin films in plasma-enhanced chemical vapor deposition (PECVD) using combination of optical emission spectroscopy (OES) and X-ray photoelectron spectroscopy (XPS). Also, experimental methods have been developed to perform scanning tunneling microscopy (STM) measurements of the surface during epitaxial growth of semiconductor layers (Voigtländer, 2001).

KMC models were initially used to develop a methodology for feedback control of thin film surface roughness (Lou and Christofides, 2003a,b). The method was successfully applied to control surface roughness in a gallium arsenide (GaAs) deposition process model (Lou and Christofides, 2004) and to control complex deposition processes including multiple components with both short-range and long-range interactions (Ni and Christofides, 2005a). Furthermore, a method for computationally efficient optimization of thin film growth using coupled PDE and kMC models was developed (Varshney and Armaou, 2005). However, the fact that kMC models are not available in closed-form makes it very difficult to use them for system-level analysis and the design and implementation of model-based feedback control systems. To achieve better closed-loop performance, it is desirable to design feedback controllers on the basis of closed-form process models, which account for the stochastic nature of the microscopic events. An approach was reported in Siettos et al. (2003), Armaou et al. (2004), and Varshney and Armaou (2006) to identify linear deterministic models from outputs of kMC simulators and design controllers using linear control theory. This approach is effective in controlling macroscopic variables which are low statistical moments of the microscopic distributions (e.g., surface coverage, which is the first moment of species distribution on a lattice). However, to control higher statistical moments of the microscopic distributions, such as the surface roughness (the second moment of height distribution on a lattice) or even the microscopic configuration (such as the surface morphology), deterministic models may not be sufficient and stochastic PDE models may be needed. In this area, other results include the construction of reduced-order approximations of the master equation (Gallivan and Murray, 2004) and control of a coupled kMC and finite-difference simulation code of a copper electrodeposition process using empirical input–output models (Rusli et al., 2006).

Stochastic PDEs arise naturally in the modeling of surface morphology of ultra thin films in a variety of material preparation processes (Edwards and Wilkinson, 1982; Villain, 1991; Vvedensky et al., 1993; Cuerno et al., 1995; Lauritsen et al., 1996). Stochastic PDEs contain the surface morphology information of thin films, and thus, they may be used for the purpose of feedback controller design. For example, it has been experimentally verified that the Kardar–Parisi–Zhang (KPZ) equation (Kardar et al., 1986) can describe the evolution of the surface morphology of GaAs thin films which is consistent with the surface morphology measured by atomic force microscopy (AFM) (Ballestad et al., 2002; Kan et al., 2004).

Advanced control methods for stochastic PDEs have been developed to address the need of model-based feedback control of thin film micro-structure in industrially important material preparation processes. Specifically, methods for state feedback control of surface roughness based on linear (Lou and Christofides, 2005a, b; Ni and Christofides, 2005b) and nonlinear (Lou and Christofides, 2006) stochastic PDE process models have been developed. The methods involve the reformulation of a stochastic PDE into a system of infinite linear/nonlinear stochastic ordinary differential equations (ODEs) by using modal decomposition, derivation of a finite-dimensional approximation that captures the dominant mode contribution to the surface roughness, and state feedback controller design based on the finite-dimensional approximation. However, state feedback control assumes a full knowledge of all states of the process, which may be restrictive in certain practical applications. Therefore, there is a strong motivation to develop output feedback control methods for processes described by stochastic PDEs which utilize information from a few measurement sensors.

Furthermore, although stochastic PDE models are suitable for model-based controller design, the construction of stochastic PDE models for thin film growth and sputtering processes directly based on microscopic process rules is, in general, a very difficult task. This motivates the development of parameter estimation methods for stochastic PDEs. Compared to deterministic systems, modeling and identification of dynamical systems described by stochastic ordinary/PDEs has received relatively limited attention and most of the results focus on stochastic ODE systems. Theoretical foundations on the analysis, parametric optimization, and optimal stochastic control for linear stochastic ODE systems can be found in the early work by Åström (1970). More recently, likelihood-based methods for parameter estimation of stochastic ODE models have been developed (Bohlin and Graebe, 1995; Kristensen

et al., 2004). These methods determine the model parameters by solving an optimization problem to maximize a likelihood function or a posterior probability density function of a given sequence of measurements of a stochastic process. For many thin film growth or sputtering processes, kMC models are available, which can be conveniently used to generate multiple independent observations of the same stochastic process. Consequently, statistical moments of the state such as the expected value (first-order moment), covariance (second-order moment), and even higher-order moments, can be obtained from the data set generated by kMC simulations. Since the dynamics of the state moments of a stochastic process may be described by deterministic differential equations, the issues of parameter estimation of stochastic models could be addressed by employing parameter estimation techniques for deterministic systems. Following this idea, a systematic identification approach was developed for linear stochastic PDEs (Lou and Christofides, 2005a) and a method for construction of linear stochastic PDE models for thin film growth using first principles-based microscopic simulations was developed and applied to construct linear stochastic PDE models for thin film deposition processes in two-dimensional (2-D) lattices (Ni and Christofides, 2005b).

However, nonlinearities exist in many material preparation processes in which surface evolution can be modeled by stochastic PDEs. A typical example of such processes is the sputtering process whose surface evolution is described by the nonlinear stochastic Kuramoto–Sivashinsky equation (KSE). In a simplified setting, the sputtering process includes two types of surface micro-processes, erosion and diffusion. The nonlinearity of the sputtering process originates from the dependence of the rate of erosion on a nonlinear sputtering yield function (Cuerno et al., 1995). Available methods for identification and construction of linear stochastic PDEs require the analytical solutions of state covariances (Lou and Christofides, 2005a; Ni and Christofides, 2005b), which prevent their direct applications to nonlinear stochastic PDEs. This motivates research on the development of methods for parameter estimation of nonlinear stochastic PDE process models.

Motivated by the above, this work focuses on model parameter estimation and model-based output feedback control of surface roughness in a sputtering process which involves two surface micro-processes: atom erosion and surface diffusion. This sputtering process is simulated using a kMC simulation method and its surface height evolution can be adequately described by the stochastic KSE, a fourth-order nonlinear stochastic PDE. First, we estimate the four parameters of the stochastic KSE so that the expected surface roughness profile predicted by the stochastic KSE is close (in a least-square sense) to the profile of the kMC simulation of the same process. To perform this model parameter estimation task, we initially formulate the nonlinear stochastic KSE into a system of infinite nonlinear stochastic ODEs. A finite-dimensional approximation of the stochastic KSE is then constructed that captures the dominant mode contribution to the state and the evolution of the state covariance of the stochastic ODE system is derived. Then, a kMC simulator is used to generate representative surface snapshots during process evolution to obtain values of the state vector of the stochastic ODE system. Subsequently, the state covariance of the stochastic ODE system that corresponds to the sputtering process is computed based on the kMC simulation results. Finally, the model parameters of the nonlinear stochastic KSE are obtained by using least-squares fitting so that the state covariance computed from the stochastic KSE process model matches that computed from kMC simulations. Subsequently, we use appropriate finite-dimensional approximations of the computed stochastic KSE model to design state and output feedback controllers, which are applied to the kMC model of the sputtering process. Extensive closed-loop system simulations demonstrate that the controllers reduce the expected surface roughness by 55% compared to the corresponding values under open-loop operation.

2. Preliminaries

2.1. Process description

We consider a one-dimensional (1-D) lattice representation of a crystalline surface of a sputtering process, which includes two surface micro-processes, atom erosion and surface diffusion. The solid-on-solid assumption is made which means that no defects or overhangs are allowed to be developed in the film. The microscopic rules under which atom erosion and surface diffusion take place are as follows: a site, i, is first randomly picked among the sites of the whole lattice and the particle at the top of this site is subject to: (a) erosion with probability $0 < f < 1$ or (b) diffusion with probability $1 - f$.

If the particle at the top of site i is subject to erosion, the particle is removed from the site i with probability $P_e \cdot Y(\phi_i)$. P_e is determined as $\frac{1}{7}$ times the number of occupied sites in a box of size 3×3 centered at the site i, which is shown in' Fig. 1. There are a total of nine sites in the box. The central one is the particle to be considered for erosion (the one marked by •). Among the remaining eight sites, the site above the central site of interest must be vacant since the central site is a surface site. Therefore, only seven of the eight sites can be occupied and the maximum value of P_e is 1. $Y(\phi_i)$ is the sputtering yield function defined as follows:

$$Y(\phi_i) = y_0 + y_1\phi_i^2 + y_2\phi_i^4, \tag{1}$$

where y_0, y_1 and y_2 are constants. Following Cuerno et al., 1995, the values of y_0, y_1 and y_2 can be chosen such that

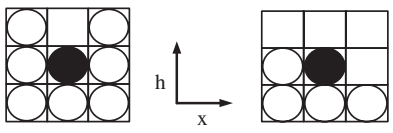

Fig. 1. Schematic of the rule to determine P_e. P_e is defined as $\frac{1}{7}$ times the number of occupied sites in a box of size 3×3 centered at the particle on the top of site i; $P_e = 1$ in the left figure and $P_e = \frac{4}{7}$ in the right figure, where the particle marked by • is on the top of site i.

$Y(0) = 0.5$, $Y(\pi/2) = 0$ and $Y(1) = 1$, which corresponds to $y_0 = 0.5$, $y_1 = 1.0065$, and $y_2 = -0.5065$. The local slope, ϕ_i, is defined as follows:

$$\phi_i = \tan^{-1}\left(\frac{h_{i+1} - h_{i-1}}{2a}\right), \tag{2}$$

where a is the lattice parameter and h_{i+1} and h_{i-1} are the values of surface height at sites $i + 1$ and $i - 1$, respectively.

If the particle at the top of site i is subject to diffusion, one of its two nearest neighbors, j ($j = i + 1$ or $i - 1$) is randomly chosen and the particle is moved to the nearest neighbor column with transition probability $w_{i\to j}$ as follows:

$$w_{i\to j} = \frac{1}{1 + \exp(\beta \Delta H_{i\to j})}, \tag{3}$$

where $\Delta H_{i\to j}$ is the energy difference between the final and initial states of the move, $\beta = 1/k_B T$ and H is defined through the Hamiltonian of an unrestricted solid-on-solid model as follows:

$$H = \left(\frac{J}{a^n}\right)\sum_{k=1}^{N}(h_k - h_{k+1})^n, \tag{4}$$

where J is the bond energy, N is the total number of sites in the lattice and n is a positive number. In the simulations presented in this paper, we use $n = 2$ and $\beta J = 2.0$ (Siegert and Plischke, 1994).

2.2. KMC model of the sputtering process

To carry out kMC simulations of this sputtering process, the rates of surface micro-processes should be computed (Fichthorn and Weinberg, 1991; Vlachos, 1997). The rates of both erosion and diffusion are site specific and can be obtained based on the process description as follows:

$$\begin{aligned} r_e(i) &= \frac{f}{\tau}\cdot P_e(i)\cdot Y(\phi_i), \\ r_d(i,j) &= \frac{1-f}{2\tau}\cdot w_{i\to j}, \end{aligned} \qquad i = 1, 2, \ldots, N, \tag{5}$$

where $r_e(i)$ is the erosion rate at site i and $r_d(i, j)$ is the rate at which a surface particle hops from site i to site j. For the sputtering process considered, only nearest neighbor hopping is allowed, so $j = i \pm 1$. $P_e(i)$ is determined by the box rule shown in Fig. 1, $Y(\phi_i)$ is defined in Eqs. (1) and (2) and $w_{i\to j}$ is defined in Eqs. (3) and (4). τ is defined as the time scale (Lauritsen et al., 1996) and is fixed at 1/s for open-loop simulations in this work.

After the rates of surface micro-processes are determined, kMC simulations can be carried out using an appropriate algorithm. In general, there are two groups of kMC algorithms which have been developed to simulate dynamical processes governed by the master equation: (a) the null-event algorithm (Ziff et al., 1986) and (b) the continuous-time Monte Carlo method (Vlachos et al., 1993). The null-event algorithm tries to execute Monte Carlo events on randomly selected sites with certain probabilities of success, while the continuous-time Monte Carlo method selects an event before the selection of the site on which the event is going to be executed. Upon a successful event, the time passed during the event is computed based on the total rates of all the micro-processes in both the null-event algorithm and the continuous-time Monte Carlo algorithm (Reese et al., 2001).

A review and analysis on complexities and efficiencies of these algorithms can be found in Reese et al. (2001). Although the continuous-time Monte Carlo algorithms with lists of neighbors and local update are often used for simulating the dynamics of complex processes, they are not appropriate for the sputtering process considered in this work. The continues-time Monte Carlo method requires the construction of a set of classes for possible Monte Carlo events and associated surface sites so that the events in each class have exactly the same transition probabilities. Typically, the transition probabilities depend on the surface micro-environment of the surface site considered. The continues-time Monte Carlo method is efficient to simulate systems such as surface reactions and thin film growth processes in which the dependence of the transition probabilities on the surface micro-environment is simply the number of nearest neighbors. This type of dependence of the transition probability on surface micro-environment results in a small number of classes needed to run the simulation. For the sputtering process considered in this work, the dependence of both the erosion and diffusion rates on the surface micro-environment is very complex and essentially all surface sites have different erosion and diffusion rates. If a set of classes are constructed so that each class contains exactly the same transition probability, a large number of classes are required, which will result in an inefficient simulation scheme. With these considerations, we decide to simulate the sputtering process in this work by using the null-event algorithm (Ziff et al., 1986) so that the complex dependence of the transition probabilities on the surface micro-configuration in the sputtering process can be handled in an efficient way.

The following kMC simulation algorithm is used to simulate the sputtering process:

- The first integer random number, ζ_1 ($0 < \zeta_1 \leqslant N$, where ζ_1 is an integer and N is the total number of surface sites) is generated to pick a site, i, among all the sites on the 1-D lattice.
- The second real random number, ζ_2 in the (0, 1) interval, is generated to decide whether the chosen site, i, is subject to erosion ($\zeta_2 < f$) or diffusion ($\zeta_2 > f$).
- If the chosen site is subject to erosion, P_e and $Y(\phi_i)$ are computed. Specifically, P_e is computed by using the box rule shown in Fig. 1 where the center of the box is the surface particle on site i and $Y(\phi_i)$ is computed by using Eqs. (1) and (2). Then, another real random number ζ_{e3} in the (0, 1) interval is generated. If $\zeta_{e3} < P_e \cdot Y(\phi_i)$ the surface particle on site i is removed. Otherwise, no event is executed.
- If the chosen site is subject to diffusion, a side neighbor, j, ($j = i + 1$ or $i - 1$ in the case of a 1-D lattice) is randomly picked and the hopping rate, $w_{i\to j}$, is computed by using Eq. (3). Then, another real random number ζ_{d3} in the (0, 1)

interval is generated. If $\zeta_{d3} < w_{i\to j}$, the surface atom is moved to the new site. Otherwise no event is executed.

- Upon the execution of an event, a time increment, δt is computed by using the following expression:

$$\delta t = -\frac{\ln \zeta_4}{\frac{f}{\tau}\sum_{i=1}^{N}[P_e(i)\cdot Y(\phi_i)] + \frac{1-f}{2\tau}\sum_{i=1}^{N}[w_{i\to i+1}+w_{i\to i-1}]}, \tag{6}$$

where ζ_4 is a real random number in the (0, 1) interval.

All random numbers, ζ_1, ζ_2, ζ_3 and ζ_4, follow a uniform probability distribution in their domains of definition.

Periodic boundary conditions (PBCs) are used in the kMC model of the sputtering process. Using PBCs, a particle that diffuses out of the simulation lattice at one boundary enters into the simulation lattice from the opposing side. Limited by the currently available computing power, the lattice size of a kMC simulation is much smaller than the size of a real process. Therefore, PBCs are widely used in molecular level simulations so that the statistical properties of a large scale stochastic process can be appropriately captured by kMC simulations carried out on a small simulation lattice (Makov and Payne, 1995).

Remark 1. Note that the probability f in Eq. (5) is dependent on the operating conditions of the sputtering process. Based on the process description, the value of f affects the ratio of erosion and diffusion events on the surface. Since an erosion event is a direct consequence of the bombardment by incoming particles, a higher bombardment rate will result in a higher erosion rate, which implies a larger f. On the other hand, the surface diffusion rate, r_d in Eq. (5), should not depend on the bombardment rate of incoming particles. When spatially distributed control is implemented, the surface bombardment rate is a spatially distributed variable. Consequently, f is a spatially distributed variable that can be computed based on the surface bombardment rate.

2.3. Stochastic PDE model of the sputtering process

The sputtering process is a stochastic process. The height fluctuations of the surface in this sputtering process can be adequately described by the stochastic KSE, which is a fourth-order, nonlinear stochastic PDE (Cuerno et al., 1995). The stochastic KSE takes the following form:

$$\frac{\partial h}{\partial t} = -\nu\frac{\partial^2 h}{\partial x^2} - \kappa\frac{\partial^4 h}{\partial x^4} + \frac{\lambda}{2}\left(\frac{\partial h}{\partial x}\right)^2 + \xi(x,t) \tag{7}$$

subject to PBCs:

$$\frac{\partial^j h}{\partial x^j}(-\pi,t) = \frac{\partial^j h}{\partial x^j}(\pi,t), \quad j = 0,\ldots,3 \tag{8}$$

and the initial condition:

$$h(x,0) = h_0(x), \tag{9}$$

where ν, κ, and λ are parameters related to surface mechanisms (Lauritsen et al., 1996), $x \in [-\pi, \pi]$ is the spatial coordinate, t is the time, $h(x,t)$ is the height of the surface at position x and time t. The PBCs are used so that the treatment of surface boundaries is consistent to that of the kMC model where PBCs are also used. $\xi(x,t)$ is a Gaussian noise with the following expressions for its mean and covariance:

$$\langle \xi(x,t)\rangle = 0,$$
$$\langle \xi(x,t)\xi(x',t')\rangle = \sigma^2\delta(x-x')\delta(t-t'), \tag{10}$$

where σ is a constant, $\delta(\cdot)$ is the Dirac function, and $\langle\cdot\rangle$ denotes the expected value.

To study the dynamics of Eq. (7), we initially consider the eigenvalue problem of the linear operator of Eq. (7), which takes the form

$$A\bar{\phi}_n(x) = -\nu\frac{\mathrm{d}^2\bar{\phi}_n(x)}{\mathrm{d}x^2} - \kappa\frac{\mathrm{d}^4\bar{\phi}_n(x)}{\mathrm{d}x^4} = \lambda_n\bar{\phi}_n(x),$$
$$\frac{\mathrm{d}^j\bar{\phi}_n}{\mathrm{d}x^j}(-\pi) = \frac{\mathrm{d}^j\bar{\phi}_n}{\mathrm{d}x^j}(+\pi), \quad j = 0,\ldots,3, \quad n = 1,\ldots,\infty, \tag{11}$$

where λ_n denotes an eigenvalue and $\bar{\phi}_n$ denotes an eigenfunction. A direct computation of the solution of the above eigenvalue problem yields $\lambda_0 = 0$ with $\psi_0 = 1/\sqrt{2\pi}$, and $\lambda_n = \nu n^2 - \kappa n^4$ (λ_n is an eigenvalue of multiplicity two) with eigenfunctions $\phi_n = (1/\sqrt{\pi})\sin(nx)$ and $\psi_n = (1/\sqrt{\pi})\cos(nx)$ for $n = 1,\ldots,\infty$. Note that the $\bar{\phi}_n$ in Eq. (11) denotes either ϕ_n or ψ_n. From the expression of the eigenvalues, it follows that for fixed values of $\nu > 0$ and $\kappa > 0$, the number of unstable eigenvalues of the operator A in Eq. (11) is finite and the distance between two consecutive eigenvalues (i.e., λ_n and λ_{n+1}) increases as n increases.

To present the method that we use to estimate the parameters of the stochastic KSE of Eq. (7) and design controllers, we first derive a nonlinear stochastic ODE approximation of Eq. (7) using Galerkin's method. To this end, we first expand the solution of Eq. (7) in an infinite series in terms of the eigenfunctions of the operator of Eq. (11) as follows:

$$h(x,t) = \sum_{n=1}^{\infty}\alpha_n(t)\phi_n(x) + \sum_{n=0}^{\infty}\beta_n(t)\psi_n(x), \tag{12}$$

where $\alpha_n(t)$, $\beta_n(t)$ are time-varying coefficients. Substituting the above expansion for the solution, $h(x,t)$, into Eq. (7) and taking the inner product with the adjoint eigenfunctions, $\phi_n^*(z) = (1/\sqrt{\pi})\sin(nz)$ and $\psi_n^*(z) = (1/\sqrt{\pi})\cos(nz)$, the following system of infinite nonlinear stochastic ODEs is obtained:

$$\frac{\mathrm{d}\alpha_n}{\mathrm{d}t} = (\nu n^2 - \kappa n^4)\alpha_n + \lambda\cdot f_{n\alpha} + \xi_\alpha^n(t),$$
$$\frac{\mathrm{d}\beta_n}{\mathrm{d}t} = (\nu n^2 - \kappa n^4)\beta_n + \lambda\cdot f_{n\beta} + \xi_\beta^n(t), \quad n = 1,\ldots,\infty, \tag{13}$$

where

$$f_{n\alpha} = \frac{1}{2}\int_{-\pi}^{\pi} \phi_n^*(x) \cdot \left(\sum_{j=1}^{\infty} \alpha_j(t) \frac{\mathrm{d}\phi_j}{\mathrm{d}x}(x) + \sum_{j=0}^{\infty} \beta_j(t) \frac{\mathrm{d}\psi_j}{\mathrm{d}x}(x) \right)^2 \mathrm{d}x,$$

$$f_{n\beta} = \frac{1}{2}\int_{-\pi}^{\pi} \psi_n^*(x) \cdot \left(\sum_{j=1}^{\infty} \alpha_j(t) \frac{\mathrm{d}\phi_j}{\mathrm{d}x}(x) + \sum_{j=0}^{\infty} \beta_j(t) \frac{\mathrm{d}\psi_j}{\mathrm{d}x}(x) \right)^2 \mathrm{d}x \tag{14}$$

and

$$\xi_\alpha^n(t) = \int_{-\pi}^{\pi} \xi(x,t)\phi_n^*(x)\,\mathrm{d}x,$$

$$\xi_\beta^n(t) = \int_{-\pi}^{\pi} \xi(x,t)\psi_n^*(x)\,\mathrm{d}x. \tag{15}$$

The covariances of $\xi_\alpha^n(t)$ and $\xi_\beta^n(t)$ can be computed by using the following result.

Result 1. If (1) $f(x)$ is a deterministic function, (2) $\eta(x)$ is a random variable with $\langle \eta(x)\rangle = 0$ and covariance $\langle \eta(x)\eta(x')\rangle = \sigma^2\delta(x-x')$, and (3) $\varepsilon = \int_a^b f(x)\eta(x)\,\mathrm{d}x$, then ε is a real random number with $\langle\varepsilon\rangle = 0$ and covariance $\langle\varepsilon^2\rangle = \sigma^2\int_a^b f^2(x)\,\mathrm{d}x$ (Åström, 1970).

Using Result 1, we obtain $\langle \xi_\alpha^n(t)\xi_\alpha^n(t')\rangle = \sigma^2\delta(t-t')$ and $\langle \xi_\beta^n(t)\xi_\beta^n(t')\rangle = \sigma^2\delta(t-t')$.

The surface roughness of the process is a variable of interest from a control point of view. The surface roughness, r, is represented by the standard deviation of the surface from its average height and is computed as follows:

$$r(t) = \sqrt{\frac{1}{2\pi}\int_{-\pi}^{\pi} [h(x,t) - \bar{h}(t)]^2\,\mathrm{d}x}, \tag{16}$$

where $\bar{h}(t) = (1/2\pi)\int_{-\pi}^{\pi} h(x,t)\,\mathrm{d}x$ is the average surface height. According to Eq. (12), we have $\bar{h}(t) = \beta_0(t)\psi_0$. Therefore, $\langle r(t)^2\rangle$ can be rewritten in terms of $\alpha_n(t)$ and $\beta_n(t)$:

$$\begin{aligned}\langle r(t)^2\rangle &= \frac{1}{2\pi}\left\langle \int_{-\pi}^{\pi} (h(x,t) - \bar{h}(t))^2\,\mathrm{d}x \right\rangle \\ &= \frac{1}{2\pi}\left\langle \int_{-\pi}^{\pi} \left[\sum_{i=1}^{\infty} \alpha_i(t)\phi_i(x) + \sum_{i=0}^{\infty} \beta_i(t)\psi_i(x) - \beta_0(t)\psi_0 \right]^2 \mathrm{d}x \right\rangle \\ &= \frac{1}{2\pi}\left\langle \int_{-\pi}^{\pi} \sum_{i=1}^{\infty} [\alpha_i(t)^2\phi_i(x)^2 + \beta_i(t)^2\psi_i(x)^2]\,\mathrm{d}x \right\rangle \\ &= \frac{1}{2\pi}\left\langle \sum_{i=1}^{\infty} (\alpha_i(t)^2 + \beta_i(t)^2) \right\rangle \\ &= \frac{1}{2\pi}\sum_{i=1}^{\infty} [\langle\alpha_i(t)^2\rangle + \langle\beta_i(t)^2\rangle]. \end{aligned} \tag{17}$$

Eq. (17) provides a direct link between the state covariance of the infinite stochastic ODEs of Eq. (13) and the expected surface roughness of the sputtering process.

Remark 2. The stochastic PDE model and the kMC model of the sputtering process are consistent. The stochastic PDE model for the sputtering processes can be derived based on the corresponding master equation, which describes the evolution of the probability that the surface is at a certain configuration (see, for example, Lauritsen et al., 1996; Vvedensky, 2003). The kMC model is a first-principle model in the sense that the microscopic events that directly form the surface are explicitly considered in the model. Mathematically, kMC simulation methods provide an unbiased realization of the master equation. Therefore, the evolution of the surface configuration predicted by the closed-form stochastic PDE model is consistent to that predicted by the kMC model. As a result, a controller designed based on the stochastic PDE process model can be applied to the kMC model of the same process (Lou and Christofides, 2005a,b, 2006; Ni and Christofides, 2005b). However, the parameters of the stochastic KSE derived based on the corresponding master equation need to be carefully estimated. A continuum limit is used in the derivation of the stochastic KSE from the master equation, which requires an infinite number of lattice sites in the kMC model. From a practical point of view, a kMC model with a finite number of lattice sites is, however, used for the simulation of the sputtering process, thereby leading to a mismatch between the stochastic KSE and the kMC model. Therefore, it is necessary to estimate the parameters of the stochastic KSE based on the kMC data directly to ensure that the KSE model predictions are close to the ones of the kMC model.

2.4. Model reduction

Owing to its infinite-dimensional nature, the system of Eq. (13) cannot be directly used as a basis for either parameter estimation or feedback controller design that can be implemented in practice (i.e., the practical implementation of such algorithms will require the computation of infinite sums which cannot be done by a computer). Instead, we will use finite-dimensional approximations of the system of Eq. (13).

Specifically, we rewrite the system of Eq. (13) as follows:

$$\frac{\mathrm{d}x_s}{\mathrm{d}t} = \Lambda_s x_s + \lambda \cdot f_s(x_s, x_f) + \xi_s,$$

$$\frac{\mathrm{d}x_f}{\mathrm{d}t} = \Lambda_f x_f + \lambda \cdot f_f(x_s, x_f) + \xi_f, \tag{18}$$

where

$$x_s = [\alpha_1 \ \cdots \ \alpha_m \ \beta_1 \ \cdots \ \beta_m]^{\mathrm{T}},$$

$$x_f = [\alpha_{m+1} \ \beta_{m+1} \ \alpha_{m+2} \ \beta_{m+2} \ \cdots]^{\mathrm{T}},$$

$$\Lambda_s = \mathrm{diag}[\lambda_1 \ \cdots \ \lambda_m \ \lambda_1 \ \cdots \ \lambda_m],$$

$$\Lambda_f = \mathrm{diag}[\lambda_{m+1} \ \lambda_{m+1} \ \lambda_{m+2} \ \lambda_{m+2} \ \cdots],$$

$$f_s(x_s, x_f) = [f_{1\alpha}(x_s, x_f) \ \cdots \ f_{m\alpha}(x_s, x_f) \ f_{1\beta}(x_s, x_f) \ \cdots \ f_{m\beta}(x_s, x_f)]^{\mathrm{T}},$$

$$f_f(x_s, x_f) = [f_{(m+1)\alpha}(x_s, x_f) \ f_{(m+1)\beta}(x_s, x_f) \ f_{(m+2)\alpha}(x_s, x_f) \ f_{(m+2)\beta}(x_s, x_f) \ \cdots]^{\mathrm{T}},$$

$$\xi_s = [\xi_\alpha^1 \ \cdots \ \xi_\alpha^m \ \xi_\beta^1 \ \cdots \ \xi_\beta^m]^{\mathrm{T}},$$

$$\xi_f = [\xi_\alpha^{m+1} \ \xi_\beta^{m+1} \ \xi_\alpha^{m+2} \ \xi_\beta^{m+2} \ \cdots]^{\mathrm{T}}. \tag{19}$$

The dimension of the x_s subsystem is $2m$ and the x_f subsystem is infinite-dimensional.

We note that the subsystem x_f in Eq. (18) is infinite-dimensional. Neglecting the x_f subsystem, the following $2m$-dimensional system is obtained:

$$\frac{\mathrm{d}\tilde{x}_s}{\mathrm{d}t} = \Lambda_s \tilde{x}_s + \lambda \cdot f_s(\tilde{x}_s, 0) + \xi_s, \tag{20}$$

where the tilde symbol in $\tilde{x}_s$ denotes that this state variable is associated with a finite-dimensional system.

3. Parameter estimation of the nonlinear stochastic PDE model

While the parameters of stochastic PDE models for several deposition and sputtering processes can be derived based on the corresponding master equation, which describes the evolution of the probability that the surface is at a certain configuration; for all practical purposes, the stochastic PDE model parameters should be estimated by matching the prediction of the stochastic PDE model to that of kMC simulations due to the approximations made in the derivation of the stochastic PDE model from the master equation (Haselwandter and Vvedensky, 2002; Lou and Christofides, 2005a).

In this section, we present a method to estimate the parameters of the nonlinear stochastic KSE model of the sputtering process by using data from the kMC simulations of the process. The parameter estimation algorithm is developed on the basis of the finite-dimensional system of Eq. (20).

3.1. System of deterministic ODEs for state covariance

The system of Eq. (20) is a finite-dimensional nonlinear stochastic ODE system including all four parameters, ν, κ, λ, and σ^2 of the stochastic KSE of Eq. (7). We first derive the system of deterministic ODEs that describes the dynamics of the covariance matrix of the state vector of Eq. (20), x_s, which is defined as $P_s = \langle x_s x_s^{\mathrm{T}} \rangle$.

Consider the evolution of the state of Eq. (20) in a small time interval, $[t, t + \Delta t]$ as follows (Kloeden and Platen, 1995; Chua et al., 2005):

$$x_s(t + \Delta t) = (I_s + \Delta t \cdot \Lambda_s) x_s(t) + \Delta t \cdot \lambda f_s(x_s(t), 0) + \Delta t \cdot \xi_s(t), \tag{21}$$

where I_s is a $2m \times 2m$ identity matrix. To study the dynamics of P_s, we approximate the Dirac function, $\delta(\cdot)$ involved in the covariances of ξ_s by $1/\Delta t$, and neglect the terms of order Δt^2. When Eq. (21) is used to compute the numerical solution of $x_s(t)$, it is clear that $x_s(t)$ is only dependent on $\xi_s(\tau)$ (for $\tau \leqslant t - \Delta t$). Since $\xi_s(t)$ and $\xi_s(\tau)$ are mutually independent according to the definition of Gaussian noise of Eq. (10) and Result 1, $\xi_s(t)$ is also independent of $x_s(t)$. We, therefore, have $\langle \xi_s(t) x_s^{\mathrm{T}}(t) \rangle = 0$ and $\langle x_s(t) \xi_s^{\mathrm{T}}(t) \rangle = 0$. Consequently, the following equation for P_s can be obtained from Eq. (21):

$$P_s(t + \Delta t) = P_s(t) + \Delta t \cdot \{\Lambda_s P_s(t) + P_s(t) \Lambda_s^{\mathrm{T}} + \lambda \langle x_s(t) f_s(x_s(t), 0)^{\mathrm{T}} + f_s(x_s(t), 0) x_s(t)^{\mathrm{T}} \rangle + R_s\}, \tag{22}$$

where R_s is the intensity of ξ_s and $R_s \delta(t - t') = \langle \xi_s(t) \xi_s^{\mathrm{T}}(t) \rangle$. In this work, $R_s = \sigma^2 I_{2m \times 2m}$.

By bringing $P_s(t)$ to the left-hand side of Eq. (22), dividing both sides by Δt and setting $\Delta t \to 0$, we obtain the following nonlinear system of deterministic ODEs for the state covariance of the system of Eq. (18):

$$\frac{\mathrm{d}P_s(t)}{\mathrm{d}t} = \Lambda_s P_s(t) + P_s(t) \Lambda_s^{\mathrm{T}} + R_s + \lambda \langle x_s(t) f_s(x_s(t), 0)^{\mathrm{T}} + f_s(x_s(t), 0) x_s(t)^{\mathrm{T}} \rangle. \tag{23}$$

Note that the linear part of Eq. (23) is the Lyapunov equation used in covariance controller design for linear systems (Hotz and Skelton, 1987). We will use this deterministic ODE system as the basis for parameter estimation.

3.2. Parameter estimation

The four parameters of the stochastic PDE process model of Eq. (7) can be estimated from Eq. (23). Specifically, the parameters ν and κ are included in the matrix Λ_s of Eq. (23) and the parameter λ is associated with the nonlinear term of Eq. (23). To this end, we need to obtain $P_s(t)$ and $\langle x_s(t) f_s(t)^{\mathrm{T}} + f_s(t) x_s(t)^{\mathrm{T}} \rangle$, which are both functions of x_s, to perform the parameter estimation.

The data of $x_s = [\alpha_1(t) \ \cdots \ \alpha_m(t) \ \beta_1(t) \ \cdots \ \beta_m(t)]^{\mathrm{T}}$ can be obtained from kMC simulations of the sputtering process.

Once x_s is obtained, $f_s(x_s,0) = [f_{1\alpha}(x_s,0)\ \cdots\ f_{m\alpha}(x_s,0)\ f_{1\beta}(x_s,0)\ \cdots\ f_{m\beta}(x_s,0)]^{\mathrm{T}}$ can be computed as follows:

$$f_{n\alpha}(x_s(t),0) = \frac{1}{2}\int_{-\pi}^{\pi}\phi_n^*(x)\left(\sum_{j=1}^{m}\alpha_j(t)\frac{\mathrm{d}\phi_j}{\mathrm{d}x}(x) + \sum_{j=0}^{m}\beta_j(t)\frac{\mathrm{d}\psi_j}{\mathrm{d}x}(x)\right)^2\mathrm{d}x, \quad n=1,2,\ldots,m,$$

$$f_{n\beta}(x_s(t),0) = \frac{1}{2}\int_{-\pi}^{\pi}\psi_n^*(x)\left(\sum_{j=1}^{m}\alpha_j(t)\frac{\mathrm{d}\phi_j}{\mathrm{d}x}(x) + \sum_{j=0}^{m}\beta_j(t)\frac{\mathrm{d}\psi_j}{\mathrm{d}x}(x)\right)^2\mathrm{d}x, \quad n=1,2,\ldots,m. \tag{24}$$

To compute the expected values for $x_s(t)\cdot x_s(t)^{\mathrm{T}}$ and $x_s(t)f_s(x_s,0)^{\mathrm{T}} + f_s(x_s,0)x_s(t)$, multiple kMC simulation runs for the sputtering process should be performed and the profiles of $x_s(t)\cdot x_s(t)^{\mathrm{T}}$ and $x_s(t)f_s(x_s,0)^{\mathrm{T}} + f_s(x_s,0)x_s(t)$ should be averaged to obtain the expected values.

The time derivative of $P_s(t)$ can be computed by the first-order approximation ($O(\Delta t)$) of the time derivative as follows:

$$\frac{\mathrm{d}P_s(t)}{\mathrm{d}t} = \frac{P_s(t+\Delta t) - P_s(t)}{\Delta t}, \tag{25}$$

where Δt is a small time interval.

When the values of $\mathrm{d}P_s(t)/\mathrm{d}t$, $P_s(t)$ and $\langle x_s(t)f_s(x_s,0)^{\mathrm{T}} + f_s(x_s,0)x_s(t)^{\mathrm{T}}\rangle$ are obtained through kMC simulation runs at a set of discrete time instants ($t=t_1, t_2, \ldots, t_k$), Eq. (23) becomes a system of linear algebraic equations for the four unknown model parameters. When the number of equations is larger than the number of parameters to be estimated, the least-squares method can be used to determine the model parameters.

Since P_s is a diagonally dominant matrix (see simulation part for a numerical verification), to make the parameter estimation algorithm insensitive to round-off errors, we propose to formulate the system of algebraic equations for least-squares fitting of the model parameters by using only the diagonal elements of the system of Eq. (23). The system of ODEs corresponding to the diagonal elements of Eq. (23) is as follows:

$$\frac{\mathrm{d}\langle\alpha_n^2(t)\rangle}{\mathrm{d}t} = 2(\nu n^2 - \kappa n^4)\cdot\langle\alpha_n^2(t)\rangle + 2\lambda\cdot\langle\alpha_n(t)\cdot f_{n\alpha}(t)\rangle + \sigma^2, \quad n=1,\ldots,m,$$

$$\frac{\mathrm{d}\langle\beta_n^2(t)\rangle}{\mathrm{d}t} = 2(\nu n^2 - \kappa n^4)\cdot\langle\beta_n^2(t)\rangle + 2\lambda\cdot\langle\beta_n(t)\cdot f_{n\beta}(t)\rangle + \sigma^2, \quad n=1,\ldots,m. \tag{26}$$

The system of Eq. (26) is a linear system with respect to ν, κ, λ and σ^2 and it is straightforward to reformulate Eq. (26) in the form of the following linear system to estimate ν, κ, λ and σ^2 using the least-squares method:

$$b = A\theta, \tag{27}$$

where $\theta = [\nu\ \kappa\ \lambda\ \sigma^2]^{\mathrm{T}}$ and

$$b = [b_1\quad b_2\quad \cdots\quad b_k]^{\mathrm{T}}$$

$$b_i = \left[\frac{\mathrm{d}\langle\alpha_1^2(t_i)\rangle}{\mathrm{d}t}\ \cdots\ \frac{\mathrm{d}\langle\alpha_m^2(t_i)\rangle}{\mathrm{d}t}\ \frac{\mathrm{d}\langle\beta_1^2(t_i)\rangle}{\mathrm{d}t}\ \cdots\ \frac{\mathrm{d}\langle\beta_m^2(t_i)\rangle}{\mathrm{d}t}\right]^{\mathrm{T}}, \quad i=1,2,\ldots,k \tag{28}$$

and

$$A = \begin{bmatrix} 2\cdot1^2\cdot\langle\alpha_1^2(t_1)\rangle & 2\cdot1^4\cdot\langle\alpha_1^2(t_1)\rangle & 2\langle\alpha_1(t_1)\cdot f_{1\alpha}(t_1)\rangle & 1\\ \vdots & \vdots & \vdots & \vdots\\ 2\cdot m^2\cdot\langle\alpha_m^2(t_1)\rangle & 2\cdot m^4\cdot\langle\alpha_m^2(t_1)\rangle & 2\langle\alpha_m(t_1)\cdot f_{m\alpha}(t_1)\rangle & 1\\ 2\cdot1^2\cdot\langle\beta_1^2(t_1)\rangle & 2\cdot1^4\cdot\langle\beta_1^2(t_1)\rangle & 2\langle\beta_1(t_1)\cdot f_{1\beta}(t_1)\rangle & 1\\ \vdots & \vdots & \vdots & \vdots\\ 2\cdot m^2\cdot\langle\beta_m^2(t_1)\rangle & 2\cdot m^4\cdot\langle\beta_m^2(t_1)\rangle & 2\langle\beta_m(t_1)\cdot f_{m\beta}(t_1)\rangle & 1\\ \vdots & \vdots & \vdots & \vdots\\ 2\cdot1^2\cdot\langle\alpha_1^2(t_k)\rangle & 2\cdot1^4\cdot\langle\alpha_1^2(t_k)\rangle & 2\langle\alpha_1(t_k)\cdot f_{1\alpha}(t_k)\rangle & 1\\ \vdots & \vdots & \vdots & \vdots\\ 2\cdot m^2\cdot\langle\alpha_m^2(t_k)\rangle & 2\cdot m^4\cdot\langle\alpha_m^2(t_k)\rangle & 2\langle\alpha_m(t_k)\cdot f_{m\alpha}(t_k)\rangle & 1\\ 2\cdot1^2\cdot\langle\beta_1^2(t_k)\rangle & 2\cdot1^4\cdot\langle\beta_1^2(t_k)\rangle & 2\langle\beta_1(t_k)\cdot f_{1\beta}(t_k)\rangle & 1\\ \vdots & \vdots & \vdots & \vdots\\ 2\cdot m^2\cdot\langle\beta_m^2(t_k)\rangle & 2\cdot m^4\cdot\langle\beta_m^2(t_k)\rangle & 2\langle\beta_m(t_k)\cdot f_{m\beta}(t_k)\rangle & 1 \end{bmatrix}. \tag{29}$$

Note that all elements in b and A can be obtained through the kMC simulations of the thin film growth or sputtering process. The least-squares fitting of the model parameters can be obtained as follows:

$$\hat{\theta} = (A^{\mathrm{T}}A)^{-1}A^{\mathrm{T}}\cdot b. \tag{30}$$

Remark 3. Different values of m are used in parameter estimation and controller design. For parameter estimation, the value of m should be large enough so that the finite-dimensional system of Eq. (27) includes all representative modes of the system. While for controller design, the value of m depends on the process and the requirement on the closed-loop performance. Specifically, m should be equal or larger than the number of unstable modes of the process to ensure closed-loop stability. Furthermore, according to Theorem 1 in Lou and Christofides, 2006, m should be large enough to have a sufficiently small ε so that the closed-loop surface roughness of the infinite-dimensional system is sufficiently close to the set-point value. However, a very large m should be avoided, since it requires a large number of actuators which may not be practical from a practical implementation point of view.

Remark 4. Note that it is important to appropriately collect the data set of surface snapshots from kMC simulations for parameter estimation. The data set should be representative so that the dynamics of the stochastic process can be adequately captured by the data set and reliable parameter estimation results can be obtained. Specifically, the condition number of the square matrix $A^{\mathrm{T}}A$ of Eq. (30) should be used as an indicator of the quality of the data set. The matrix A is constructed by using the data derived from the surface snapshots. The condition number measures the sensitivity of the solution to the perturbations in A and b. There is stochastic noise contained in the

data used to construct the matrix A and the vector b in Eq. (30). This noise will perturb A and b from their true values. A low condition number of the square matrix $A^{\mathrm{T}}A$ will ensure that the perturbations in A and b introduced by the noise will not result in significant errors in the estimated model parameters. According to the simulations, a low condition number between 10 and 20 can be achieved by appropriately selecting snapshots while a large condition number could be over 1000. Another good and practical criterion for a given situation is to compare the profiles of the expected surface roughness of the process and the stochastic PDE with estimated parameters. If they are matched consistently, the condition number of $A^{\mathrm{T}}A$ is considered as a low number for that particular problem. The sampling time and the number of surface snapshots should be carefully selected so that the condition number of the square matrix $A^{\mathrm{T}}A$ is small. Another effective way to decrease the condition number is to acquire as many representative surface snapshots of the process as possible, e.g., with different initial conditions.

Remark 5. Note that this work does not intent to develop a new model for the sputtering process and validate the model against experimental data from a process. Instead, the focus of this work is to estimate the parameters of a stochastic PDE model and compare the model output against that from a kMC model, which is considered as a more accurate process model. Therefore, if the kMC model for the sputtering process can capture the roughness evolution of a real process, our method results in a closed-form stochastic PDE model that possesses a very similar modeling capability. There is a large body of literature available for kMC simulations of various sputtering and thin film growth processes. Our work can be readily extended to a variety of real world processes to construct stochastic PDE process models provided that an accurate kMC model is available for the process of interest.

4. Feedback control

In this section, we design a linear output feedback controller based on the stochastic KSE process model to regulate the expected surface roughness of the sputtering process to a desired level. A state feedback controller is initially designed by following the method developed in our previous work (Lou and Christofides, 2005a). Then, a static state estimation scheme is constructed and the output feedback controller design is completed by combining the state feedback control law and the state estimation scheme.

4.1. Distributed control problem formulation

We consider the stochastic KSE with distributed control in the spatial domain $[-\pi, \pi]$:

$$\frac{\partial h}{\partial t} = -\nu\frac{\partial^2 h}{\partial x^2} - \kappa\frac{\partial^4 h}{\partial x^4} + \frac{\lambda}{2}\left(\frac{\partial h}{\partial x}\right)^2 + \sum_{i=1}^{p} b_i(x)u_i(t) + \xi(x,t) \tag{31}$$

subject to PBCs:

$$\frac{\partial^j h}{\partial x^j}(-\pi, t) = \frac{\partial^j h}{\partial x^j}(\pi, t), \quad j = 0, \ldots, 3 \tag{32}$$

and the initial condition:

$$h(x, 0) = h_0(x), \tag{33}$$

where u_i is the ith manipulated input, p is the number of manipulated inputs and b_i is the ith actuator distribution function (i.e., b_i determines how the control action computed by the ith control actuator, u_i, is distributed (e.g., point or distributed actuation) in the spatial interval $[-\pi, \pi]$). The variables are defined in the same way as in Eq. (7) of Section 2.3. Following similar derivations to the ones of Section 2.3, the following system of infinite nonlinear stochastic ODEs with distributed control can be obtained:

$$\begin{aligned}
\frac{\mathrm{d}\alpha_n}{\mathrm{d}t} &= (\nu n^2 - \kappa n^4)\alpha_n + \lambda \cdot f_{n\alpha} \\
&\quad + \sum_{i=1}^{p} b_{i\alpha_n} u_i(t) + \xi_\alpha^n(t), \quad n = 1, \ldots, \infty, \\
\frac{\mathrm{d}\beta_n}{\mathrm{d}t} &= (\nu n^2 - \kappa n^4)\beta_n + \lambda \cdot f_{n\beta} \\
&\quad + \sum_{i=1}^{p} b_{i\beta_n} u_i(t) + \xi_\beta^n(t), \quad n = 1, \ldots, \infty,
\end{aligned} \tag{34}$$

where $f_{n\alpha}$ and $f_{n\beta}$ are defined in Eq. (14) and $\xi_\alpha^n(t)$ and $\xi_\beta^n(t)$ are defined in Eq. (15). $b_{i\alpha_n}$ and $b_{i\beta_n}$ are defined as follows:

$$\begin{aligned}
b_{i\alpha_n} &= \int_{-\pi}^{\pi} \phi_n^*(x) b_i(x)\,\mathrm{d}x, \\
b_{i\beta_n} &= \int_{-\pi}^{\pi} \psi_n^*(x) b_i(x)\,\mathrm{d}x.
\end{aligned} \tag{35}$$

The system of Eq. (34) can be rewritten in the following form:

$$\begin{aligned}
\frac{\mathrm{d}x_s}{\mathrm{d}t} &= \Lambda_s x_s + f_s(x_s, x_f) + B_s u + \xi_s, \\
\frac{\mathrm{d}x_f}{\mathrm{d}t} &= \Lambda_f x_f + f_f(x_s, x_f) + B_f u + \xi_f,
\end{aligned} \tag{36}$$

where x_s, x_f, Λ_s, Λ_f, $f_s(x_s, x_f)$, $f_f(x_s, x_f)$, ξ_s and ξ_f are defined in Eq. (19), and

$$\begin{aligned}
B_s &= \begin{bmatrix} b_{1\alpha_1} & \cdots & b_{p\alpha_1} \\ \vdots & \ddots & \vdots \\ b_{1\alpha_m} & \cdots & b_{p\alpha_m} \\ b_{1\beta_1} & \cdots & b_{p\beta_1} \\ \vdots & \ddots & \vdots \\ b_{1\beta_m} & \cdots & b_{p\beta_m} \end{bmatrix}, \\
B_f &= \begin{bmatrix} b_{1\alpha_{m+1}} & \cdots & b_{p\alpha_{m+1}} \\ b_{1\beta_{m+1}} & \cdots & b_{p\beta_{m+1}} \\ b_{1\alpha_{m+2}} & \cdots & b_{p\alpha_{m+2}} \\ b_{1\beta_{m+2}} & \cdots & b_{p\beta_{m+2}} \\ \vdots & \vdots & \vdots \end{bmatrix}.
\end{aligned} \tag{37}$$

Note that the dimension of the x_s subsystem is $2m$ and the x_f subsystem is infinite-dimensional. Neglecting the x_f subsystem, the following $2m$-dimensional system is obtained:

$$\frac{d\tilde{x}_s}{dt} = \Lambda_s \tilde{x}_s + \lambda \cdot f_s(\tilde{x}_s, 0) + B_s u + \xi_s, \tag{38}$$

where the tilde symbol in $\tilde{x}_s$ denotes that this state variable is associated with a finite-dimensional system.

We note here that the accuracy of the finite-dimensional system can be improved by including a finite-number of the x_f modes using the concept of approximate inertial manifolds (Christofides and Daoutidis, 1997; Armaou and Christofides, 2002).

Remark 6. Note that in practice, the control action, u_i, can be implemented by manipulating the gas composition across the surface in either a deposition process or a sputtering process. Spatially controllable CVD reactors have been developed to enable across-wafer spatial control of surface gas composition during deposition (Choo et al., 2005). In such a control problem formulation, the rate that particles land on the surface or the rate that surface particles are eroded is spatially distributed and is computed by the controller. The parameters of the stochastic KSE model of Eq. (31) depend on both the temperature and the rate that particles land on the surface or that surface particles are eroded (Lauritsen et al., 1996). In this work, the temperature is assumed to be a constant. The rate that particles land on the surface or the rate that surface particles are eroded used to compute the stochastic KSE model parameters corresponds to that under open-loop operation, and thus, it is also a constant. The contribution of the spatially distributed rate that particles land on the surface or the rate that surface particles are eroded to the fluctuations of the surface height profile (e.g., the surface roughness) is captured by the term $\sum_{i=1}^{p} b_i(x)u_i(t)$. This control problem formulation is further supported by our simulation results which demonstrate that the controller designed on the basis of the stochastic KSE model of a sputtering process can be successfully applied to the kMC model of the same sputtering process to control the surface roughness to desired levels (see simulation results section).

4.2. State feedback control

Following the method presented in Lou and Christofides (2005a), we design a linear state feedback controller on the basis of the linearization of Eq. (38) around its zero solution. To simplify our development, we assume that $p = 2m$ (i.e., the number of control actuators is equal to the dimension of the finite-dimensional system) and pick the actuator distribution functions such that B_s^{-1} exists. The linear state feedback control law then takes the form

$$u = B_s^{-1}(\Lambda_{cs} - \Lambda_s)\tilde{x}_s, \tag{39}$$

where the matrix Λ_{cs} contains the desired poles of the closed-loop system; $\Lambda_{cs} = \mathrm{diag}[\lambda_{c\alpha 1} \cdots \lambda_{c\alpha m}\ \lambda_{c\beta 1} \cdots \lambda_{c\beta m}]$, $\lambda_{c\alpha i}$ and $\lambda_{c\beta i}$ $(1 \leqslant i \leqslant m)$ are desired poles of the closed-loop finite-dimensional system, which satisfy $\mathrm{Re}\{\lambda_{c\alpha i}\} < 0$ and $\mathrm{Re}\{\lambda_{c\beta i}\} < 0$ for $(1 \leqslant i \leqslant m)$ and can be determined from the desired closed-loop surface roughness level.

4.3. Output feedback control

The state feedback controller of Eq. (39) was derived under the assumption that measurements of the states $\tilde{x}_s$ are available, which implies that measurements of the surface height profile, $h(x,t)$, are available at all positions and time. However, from a practical point of view, measurements of the surface height profile are only available at a finite number of spatial positions. Motivated by this practical consideration, we address in this section the synthesis of an output feedback controller that uses measurements of the thin film surface height at distinct locations to enforce a desired surface roughness in the closed-loop kMC simulation model. The measured surface height profile can be expressed as follows:

$$y(t) = [h(x_1,t)\ \ h(x_2,t)\ \ \cdots\ \ h(x_q,t)]^{\mathrm{T}}, \tag{40}$$

where x_i $(i = 1, 2, \ldots, q)$ denotes a location of a point measurement sensor and q is the number of measurement sensors. Since the height profile $h(x,t)$ can be expanded into an infinite series as shown in Eq. (12), the vector of output measurements of Eq. (40) can be written in terms of the state of the infinite-dimensional system, x_s and x_f, as follows:

$$\begin{aligned} y(t) &= \begin{bmatrix} \sum_{n=1}^{\infty} \alpha_n(t)\phi_n(x_1) + \sum_{n=1}^{\infty} \beta_n(t)\psi_n(x_1) + \beta_0(t)\psi_0 \\ \sum_{n=1}^{\infty} \alpha_n(t)\phi_n(x_2) + \sum_{n=1}^{\infty} \beta_n(t)\psi_n(x_2) + \beta_0(t)\psi_0 \\ \vdots \\ \sum_{n=1}^{\infty} \alpha_n(t)\phi_n(x_q) + \sum_{n=1}^{\infty} \beta_n(t)\psi_n(x_q) + \beta_0(t)\psi_0 \end{bmatrix} \\ &= C_s \begin{bmatrix} \beta_0(t) \\ x_s(t) \end{bmatrix} + C_f x_f(t), \end{aligned} \tag{41}$$

where

$$C_s(t) = \begin{bmatrix} \psi_0 & \phi_1(x_1) & \phi_2(x_1) & \cdots & \phi_m(x_1) & \psi_1(x_1) & \psi_2(x_1) & \cdots & \psi_m(x_1) \\ \psi_0 & \phi_1(x_2) & \phi_2(x_2) & \cdots & \phi_m(x_2) & \psi_1(x_2) & \psi_2(x_2) & \cdots & \psi_m(x_2) \\ \vdots & \vdots & \vdots & \ddots & \vdots & \vdots & \vdots & \ddots & \vdots \\ \psi_0 & \phi_1(x_q) & \phi_2(x_q) & \cdots & \phi_m(x_q) & \psi_1(x_q) & \psi_2(x_q) & \cdots & \psi_m(x_q) \end{bmatrix},$$

$$C_f(t) = \begin{bmatrix} \phi_{m+1}(x_1) & \psi_{m+1}(x_1) & \phi_{m+2}(x_1) & \psi_{m+2}(x_1) & \cdots \\ \phi_{m+1}(x_2) & \psi_{m+1}(x_2) & \phi_{m+2}(x_2) & \psi_{m+2}(x_2) & \cdots \\ \vdots & \vdots & \ddots & & \\ \phi_{m+1}(x_q) & \psi_{m+1}(x_q) & \phi_{m+2}(x_q) & \psi_{m+2}(x_q) & \cdots \end{bmatrix}. \tag{42}$$

Neglecting the x_f component in the system of Eqs. (36) and (41) and linearizing the resulting finite-dimensional system around its zero solution, the following linearized finite-dimensional system is obtained:

$$\frac{d\tilde{x}_s}{dt} = \Lambda_s \tilde{x}_s + B_s u + \xi_s,$$
$$\tilde{y} = C_s \begin{bmatrix} \tilde{\beta}_0 \\ \tilde{x}_s \end{bmatrix}. \quad (43)$$

The system of Eq. (43) is used for the output feedback control design. The general form of the static output feedback control laws is as follows:

$$u = \mathscr{F}(y), \quad (44)$$

where $\mathscr{F}(y)$ is a vector function and y is the vector of measured outputs. The synthesis of the controller of Eq. (44) will be achieved by combining the state feedback controller of Eq. (39) with a procedure proposed in Christofides and Baker (1999) for obtaining estimates for the states of the approximate ODE model of Eq. (43) from the measurements. To this end, we need to impose the following requirement on the number of measurements in order to obtain estimates of the states x_s of the finite-dimensional system of Eq. (38) from the measurements y.

Assumption 1. *$q = 2m+1$, and the inverse of C_s exists, so that $[\hat{\beta}_0 \ \hat{x}_s^T]^T = C_s^{-1} y$, where $\hat{\beta}_0$ and $\hat{x}_s$ denote the estimates of β_0 and x_s from the output y, respectively.*

We note that the requirement that the inverse of C_s exists can be achieved by appropriate choice of the location of the measurement sensors. When point measurement sensors are used, this requirement can be verified by checking the invertibility of the matrix.

The output feedback control law of Eq. (44) is designed on the basis of Eq. (43) as follows:

$$u = \mathscr{F}(y) = B_s^{-1}(\Lambda_{cs} - \Lambda_s)[\mathbf{0} \ \ I_s] C_s^{-1} y, \quad (45)$$

where $[\mathbf{0} \ I_s]$ is used to extract estimated states x_s from $\begin{bmatrix} \hat{\beta}_0 \\ \hat{x}_s \end{bmatrix}$, $\mathbf{0}$ is a $2m \times 2m$ zero matrix and I_s is a $2m \times 2m$ elementary matrix.

Remark 7. Note that although the stochastic KSE model of Eq. (7) for which we computed the parameters is a nonlinear model for the sputtering process, the state feedback controller of Eq. (39) and the output feedback controller of Eq. (45) are linear controllers that are designed based on a linearization of the stochastic KSE around its zero solution. Our decision to identify the nonlinear stochastic KSE model of the sputtering process but design the output feedback controller based on a linearized process model is made based on two considerations. First, from a modeling point of view, the sputtering process is a nonlinear process and a linear model is not sufficient to represent the time evolution of the surface height profile. Specifically, due to the existence of unstable eigenvalues of the linear operator of Eq. (11), the expected surface roughness predicted by a linear stochastic PDE model will go to infinity as $t \to \infty$, which is not true for the sputtering process due to the un-modeled nonlinearities of the process. Therefore, it is important to model the sputtering process using a nonlinear stochastic PDE model to appropriately capture the process dynamics. On the other hand, since the instability of the spatially uniform steady state comes from the linear part of the model, and the nonlinear part of the stochastic KSE helps bound the surface roughness, for control purposes, we only need to focus on the stabilization of the linear part of the stochastic KSE. This argument can be further supported by our simulation results, which demonstrate the effectiveness of the linear output feedback controller designed in this work.

Remark 8. We note that a full-scale model of a sputtering process would consist of a 2-D lattice representation of the surface. Although we developed the method for output feedback control design based on a 1-D lattice representation of the surface, it is possible to extend the proposed method to control the surface roughness of material preparation processes taking place in 2-D domains. In a 2-D in space process, the feedback control design will be based on a 2-D extension of the model of Eq. (36). Moreover, Eq. (36) will be obtained by solving the eigenvalue/eigenfunction problem in the 2-D spatial domain subject to appropriate boundary conditions; this can be achieved in a similar way to that followed for the 1-D spatial domain (see the work by Ni and Christofides, 2005b for results on the solution of the eigenvalue/eigenfunction problem for a 2-D spatial domain). Once the modal representation of Eq. (36) corresponding to the 2-D stochastic PDE model is obtained, the method proposed in this work for controller design can be applied to control the surface roughness.

5. Numerical simulations

In this section, we present applications of the proposed model parameter estimation method and both of the state feedback and output feedback controllers to the kMC model of a sputtering process to demonstrate the effectiveness of the algorithms. Specifically, the model parameters of the stochastic KSE process model are first estimated by using data of surface snapshots obtained form kMC simulations. The identified KSE model is linearized and is consequently used as a basis for both state feedback control and output feedback control design. The controllers designed based on the stochastic KSE model are applied to the kMC model of the sputtering process to reduce the expected surface roughness to desired levels.

In all simulations, we consider a sputtering process that takes place on a lattice containing 200 sites. Therefore, $a = 0.0314$. The sputtering yield function, $Y(\phi_i)$ is a nonlinear function of ϕ_i, which takes the form of Eq. (1). y_0, y_1 and y_2 are chosen such that $Y(0) = 0.5$, $Y(\pi/2) = 0$ and $Y(1) = 1$ (Cuerno et al., 1995).

5.1. Model parameter estimation

We first compute the profiles of the state covariance and the expected values for $\alpha_n \cdot f_{n\alpha}$ and $\beta_n \cdot f_{n\beta}$ from kMC simulations

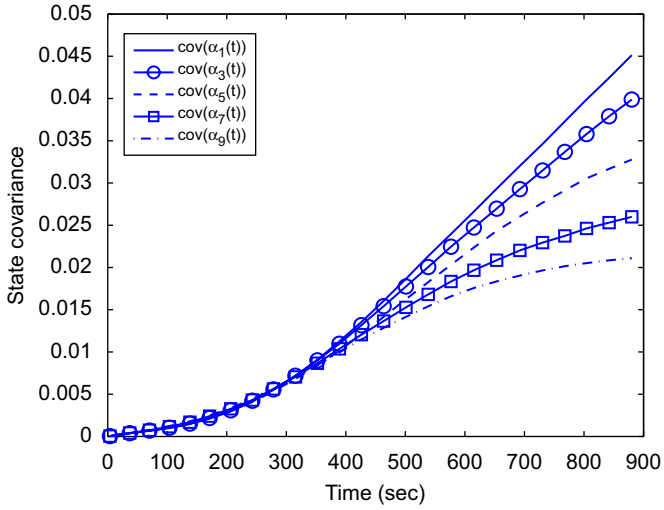

Fig. 2. Profiles of the state covariance $\langle \alpha_n^2(t) \rangle$ for $n = 1, 3, 5, 7$, and 9.

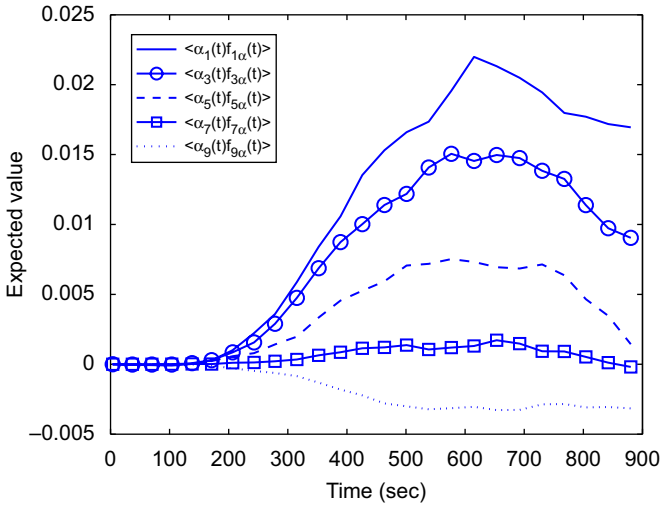

Fig. 3. Profiles of the expected value for $\alpha_n \cdot f_{n\alpha}(t)$ for $n = 1, 3, 5, 7$, and 9.

of the sputtering process. Upon the execution of an event, the state of the stochastic KSE model (α_n or β_n) is updated. If the executed event is erosion, α_n or β_n can be updated as follows (Lou and Christofides, 2005a, 2006):

$$\alpha_n^{\text{new}} = \alpha_n^{\text{old}} + \frac{a[\psi(n, z_i - a/2) - \psi(n, z_i + a/2)]}{n},$$
$$\beta_n^{\text{new}} = \beta_n^{\text{old}} + \frac{a[\phi(n, z_i + a/2) - \phi(n, z_i - a/2)]}{n}. \quad (46)$$

If the executed event is diffusion from site i to site j, α_n or β_n are updated as follows:

$$\alpha_n^{\text{new}} = \alpha_n^{\text{old}} + \frac{a}{n} \cdot \{[\psi(n, z_i - a/2) - \psi(n, z_i + a/2)] - [\psi(n, z_j - a/2) - \psi(n, z_j + a/2)]\},$$
$$\beta_n^{\text{new}} = \beta_n^{\text{old}} + \frac{a}{n} \cdot \{[\phi(n, z_i + a/2) - \phi(n, z_i - a/2)] - [\phi(n, z_j + a/2) - \phi(n, z_j - a/2)]\}, \quad (47)$$

where a is the lattice parameter and z_i is the coordinate of the center of site i.

The terms $\alpha_n \cdot f_{n\alpha}$ and $\beta_n \cdot f_{n\beta}$ are computed by using Eq. (24) with $m = 10$ for $n = 1, 2, \ldots, 10$. The expected profiles are the averages of profiles obtained from 10 000 independent kMC simulation runs. The covariance profiles of α_1, α_3, α_5, α_7, and α_9 are shown in Fig. 2 and the profiles for the expected values of $\alpha_1 f_{1\alpha}$, $\alpha_3 f_{3\alpha}$, $\alpha_5 f_{5\alpha}$, $\alpha_7 f_{7\alpha}$, and $\alpha_9 f_{9\alpha}$ are shown in Fig. 3. Similar profiles are observed for the covariance of β_n and $\beta_n f_{n\beta}$, and are omitted here for brevity.

Since we use $m = 10$, the first $2m = 20$ modes are used for parameter estimation. The three-dimensional profile of the covariance matrix for the first 20 states at the end of a simulation run is plotted in Fig. 4. It is clear that the covariance matrix is diagonally dominant. Therefore, it is appropriate to use just the diagonal elements of the system of Eq. (23) for parameter estimation so that the estimation algorithm is insensitive to round-off errors. To formulate the least-squares fitting problem,

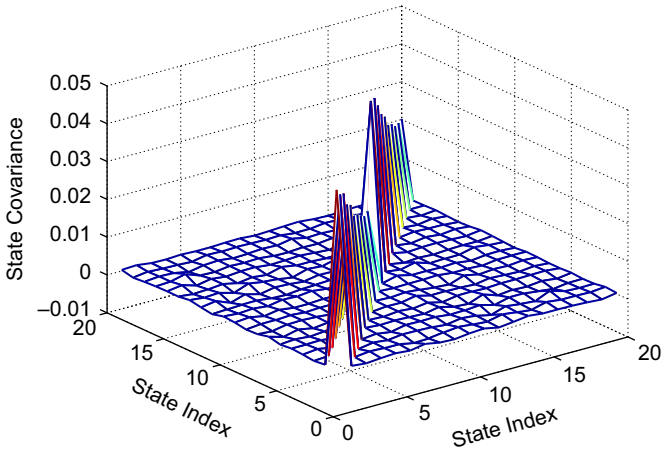

Fig. 4. The covariance matrix for the first 20 states: a diagonally dominant matrix.

$\mathrm{d}\langle \alpha_n^2(t) \rangle / \mathrm{d}t$, $\mathrm{d}\langle \beta_n^2(t) \rangle / \mathrm{d}t$, $\langle \alpha_n^2(t) \rangle$, $\langle \beta_n^2(t) \rangle$, $\langle \alpha_n(t) \cdot f_{n\alpha}(t) \rangle$, and $\langle \beta_n(t) \cdot f_{n\beta}(t) \rangle$ are evaluated at the first 150 available discrete time instants in the data obtained from kMC simulations. Therefore, in the least-squares fitting formulations of Eqs. (27) and (30), A is a 3000×4 matrix, b is a 3000×1 vector and $\theta = [\nu \ \kappa \ \lambda \ \sigma^2]^{\mathrm{T}}$. The values of the four parameters obtained from least-squares fitting are $\nu = 2.76 \times 10^{-5}$, $\kappa = 1.54 \times 10^{-7}$, $\lambda = 3.06 \times 10^{-3}$, and $\sigma^2 = 1.78 \times 10^{-5}$.

To validate the parameter estimation method, we first compute the expected open-loop surface roughness from the stochastic KSE model of Eq. (7) with the computed parameters. Then, the profile from the stochastic KSE with computed parameters is compared to that from the kMC model. The expected surface roughness is computed from the simulations of the stochastic KSE and the kMC model by averaging surface roughness profiles obtained from 100 and 10 000 independent runs, respectively. The simulation result is shown in Fig. 5. It is clear that the computed model parameters result in consistent expected surface roughness profiles from the stochastic

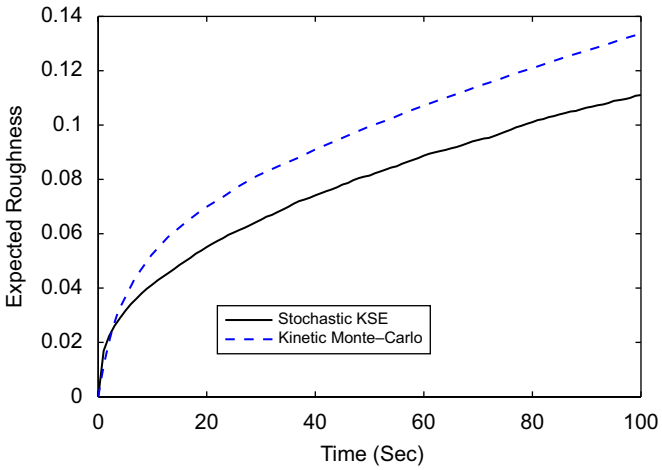

Fig. 5. Comparison of the open-loop profile of the expected surface roughness of the sputtering process from the kMC simulator and that from the solution of the stochastic KSE using the estimated parameters.

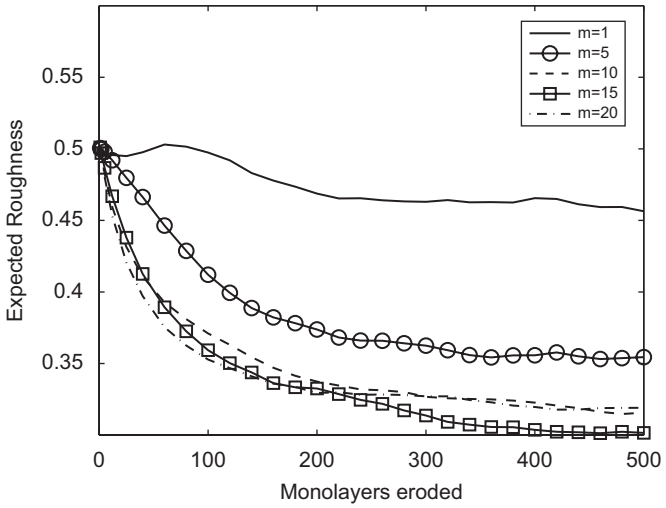

Fig. 6. Closed-loop surface roughness profiles in the sputtering process under state feedback control with different m: initial surface roughness is 0.5.

KSE model of Eq. (7) and from the kMC simulator of the sputtering process. There is observable difference between the two profiles, which indicates the existence of a slight mismatch of the identified model with the kMC model of the sputtering process. The mismatch between the profiles originates from the fact that the KSE model is derived from the master equation of the sputtering process with an assumption of infinitesimal lattice size, while in the kMC simulation a 200-lattice (finite-numbered) model is used.

5.2. Closed-loop simulation under state feedback control

We design a state feedback controller for the sputtering process based on the $2m$-order approximation of the stochastic ODE and apply the controller to the kMC model of the sputtering process to control the surface roughness to the desired level. The state feedback controller is designed using the computed KSE model parameters and $\Lambda_{cs} = \text{diag}[-0.01\ -0.01\ \cdots\ -0.01]$. $2m$ control actuators are used to control the system. The ith actuator distribution function is taken to be

$$b_i(z) = \begin{cases} \dfrac{1}{\sqrt{\pi}} \sin(iz), & i = 1, \ldots, m, \\ \dfrac{1}{\sqrt{\pi}} \cos[(i-m)z], & i = m+1, \ldots, 2m. \end{cases} \tag{48}$$

The controller is implemented by manipulating the probability that a randomly selected site is subject to the erosion rule, f. From a practical point of view, a spatially distributed erosion probability can be realized by varying the gas composition across the substrate. Specifically, the bombardment rate of each surface site under feedback control is $1/\tau = 1 + (\sum_{j=1}^{2m} b_j(z_i)u_j(t))/a$. Since the variation of the bombardment rate does not change the surface diffusion rate, according to the discussion in Remark 1, the f of site i should relate to the surface bombardment rate in a way that $(1-f)/\tau$ is a constant. Since in open-loop operation, $\bar{f} = 0.5$ and $1/\bar{\tau} = 1$, we

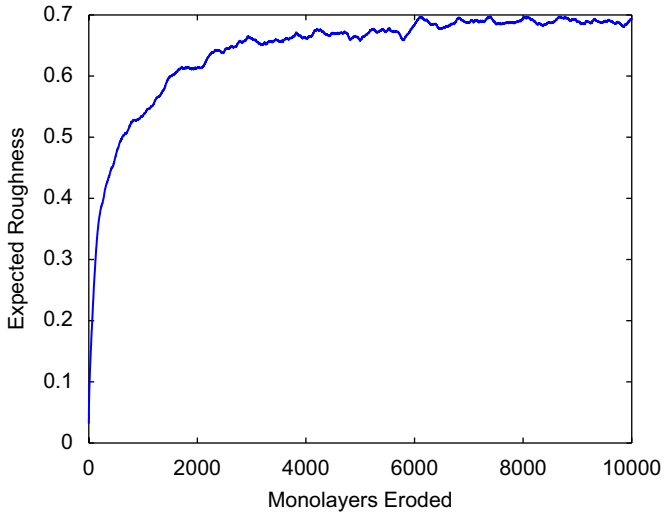

Fig. 7. Open-loop expected surface roughness profile of the sputtering process.

have $(1-f)/\tau = (1-\bar{f})/\bar{\tau} = 0.5$. Therefore, f under feedback control is determined according to the following expression:

$$f(i) = \frac{\bar{f} + (\sum_{j=1}^{2m} b_j(z_i)u_j(t))/a}{1 + (\sum_{j=1}^{2m} b_j(z_i)u_j(t))/a}, \tag{49}$$

where $\bar{f} = 0.5$ is the probability a selected surface site is subject to erosion and $1/\bar{\tau} = 1$ is the bombardment rate of each surface site in open-loop operation.

The simulation algorithm used to run the kMC simulations for the closed-loop system is similar to the one for the open-loop system except that once an event is executed, the first $2m$ states ($\alpha_1, \ldots, \alpha_m$ and $\beta_1, \ldots, \beta_m$) are updated and new control actions are computed to update the value of f (defined in Eq. (49)) for each surface site.

The dimension of the reduced-order model, $2m$, needs to be appropriately determined. It should be large enough so that all

unstable modes are included. The number of unstable modes is 26 according to the estimated model parameters of the sputtering process considered in this work. When $2m \geqslant 26$ and the desired closed-loop poles are negative, the linearized closed-loop system under the state feedback control is stable. This is demonstrated by the simulation result with $2m = 40$.

The closed-loop system simulation result under the state feedback controller designed on the basis of a 40th-order approximation is shown in Fig. 6 (the dash-dotted line labeled with $m = 20$). The other profiles in Fig. 6 are under controllers of different orders and will be discussed later. The initial surface roughness is around 0.5. The expected surface roughness is computed by averaging the surface roughness profiles obtained from 100 independent runs. It is clear from Fig. 6 that the state feedback controller effectively reduces the expected surface roughness and stabilizes it at about 0.3. For the purpose of comparison, an expected open-loop surface roughness profile, which is obtained by averaging 100 independent open-loop simulation runs, is shown in Fig. 7. Under open-loop operation, the final steady-state surface roughness is around 0.7. Therefore, the state feedback controller reduces the expected surface roughness by 55%. This demonstrates the effectiveness of the state feedback control law. A snapshot of the surface configuration at the end of the closed-loop simulation is shown in Fig. 9.

However, even when the size of the reduced-order system is smaller than the number of the unstable modes, the state feedback control law still reduces the surface roughness compared to the open-loop value. This is due to the nonlinearity of the stochastic KSE, which bounds the unstable linear terms and prevents the expected surface roughness from

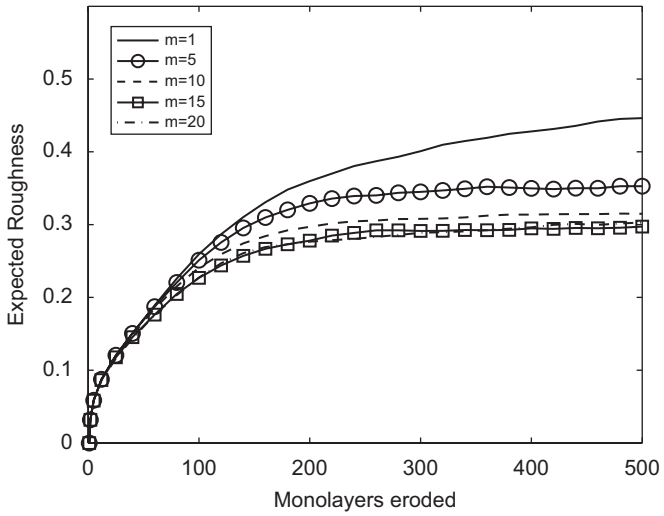

Fig. 8. Closed-loop surface roughness profiles in the sputtering process under state feedback control with different m: flat initial surface.

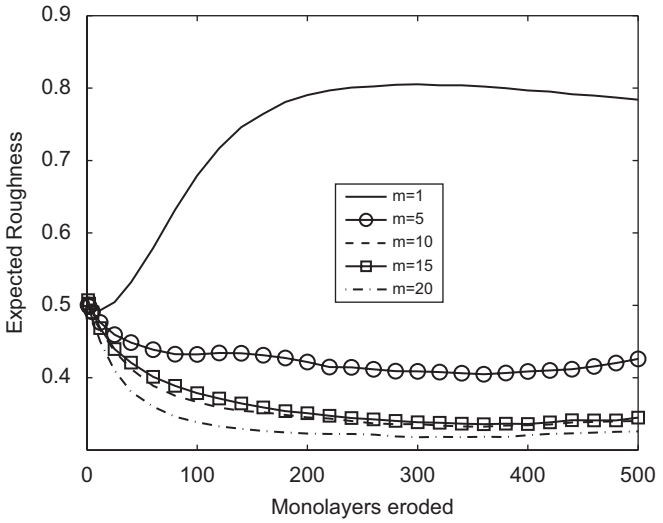

Fig. 10. Closed-loop surface roughness profiles in the sputtering process under output feedback control with different m: initial surface roughness is 0.5.

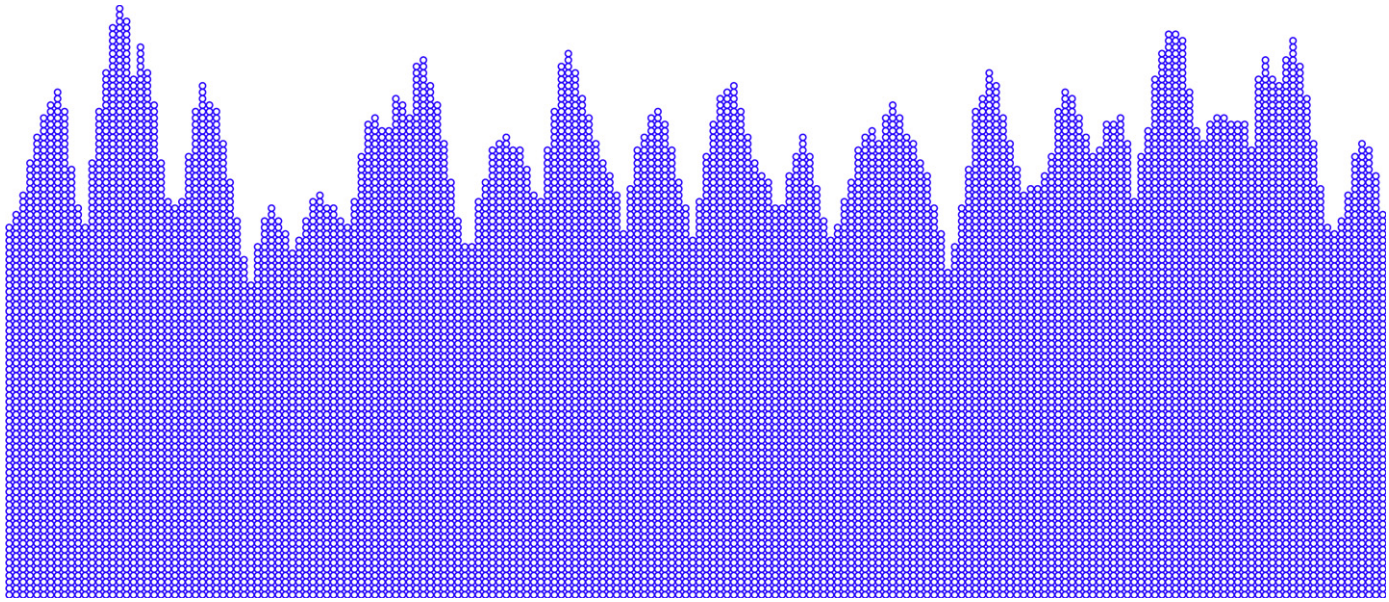

Fig. 9. A snapshot of the surface configuration at the end of the closed-loop simulation under the 40th-order state feedback controller: initial surface roughness is 0.5.

going to infinity. To demonstrate this and show that $m = 20$ is appropriate for the state feedback controller design, we compare several state feedback controllers based on the reduced-order systems with different dimensions, $m = 1$, 5, 10, 15 as well as $m = 20$. For each controller, the number of actuators is the same with the dimension of the reduced-order system and $\Lambda_{cs} = \text{diag}[-0.01 \quad -0.01 \quad \cdots \quad -0.01]$. The expected surface roughness is the average of the surface roughness profiles obtained from 100 independent runs. The initial surface roughness for the closed-loop simulation is fixed at 0.5 and 0.0, separately.

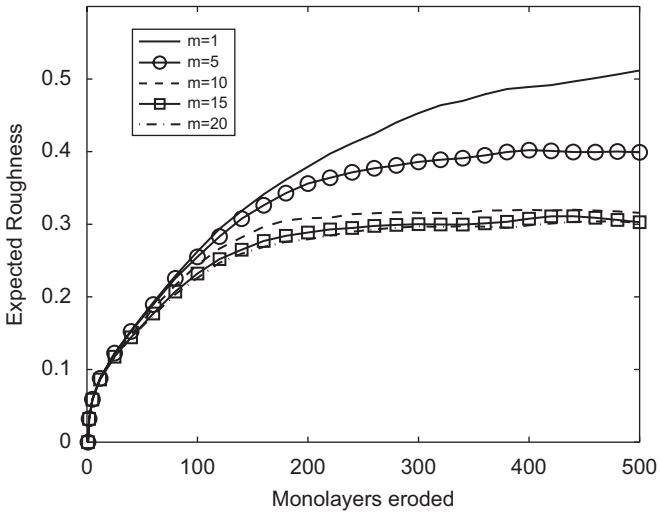

Fig. 11. Closed-loop surface roughness profiles in the sputtering process under output feedback control with different m: flat initial surface.

The closed-loop simulation results are shown in Figs. 6 and 8. Despite the use of different initial conditions, the expected surface roughness profiles of the closed-loop systems under the various state feedback controllers are stabilized at the same values, for the same m. It is also clear that all final expected closed-loop surface roughness values are lower compared to the open-loop simulation. The surface roughness is further reduced as m increases. However, there is no significant difference between the expected roughness of $m = 15$ and 20. Higher-order controllers will not result in further reduction of the surface roughness. So it is concluded that $m = 20$ is an appropriate dimension of the reduced-order system for the state feedback controller.

5.3. Closed-loop simulation under output feedback control

We also apply the output feedback controller of Eq. (45) to the kMC model of the sputtering process. The output feedback controller is designed based on the same order stochastic ODE approximation used in the design of the state feedback controller in Section 5.2. The positions of point measurements are evenly distributed on the surface lattice. The same control actuators are used to control the system as defined in Eq. (48).

The closed-loop system simulation result under the 40th-order output feedback controller is shown in Fig. 10 (the dash-dotted line labeled with $m = 20$). The expected surface roughness is the average of surface roughness profiles obtained from 100 independent runs. The initial surface roughness is fixed at 0.5. Similar to the closed-loop simulation result under state feedback control, the output feedback controller also reduces the expected surface roughness by 55% compared to the

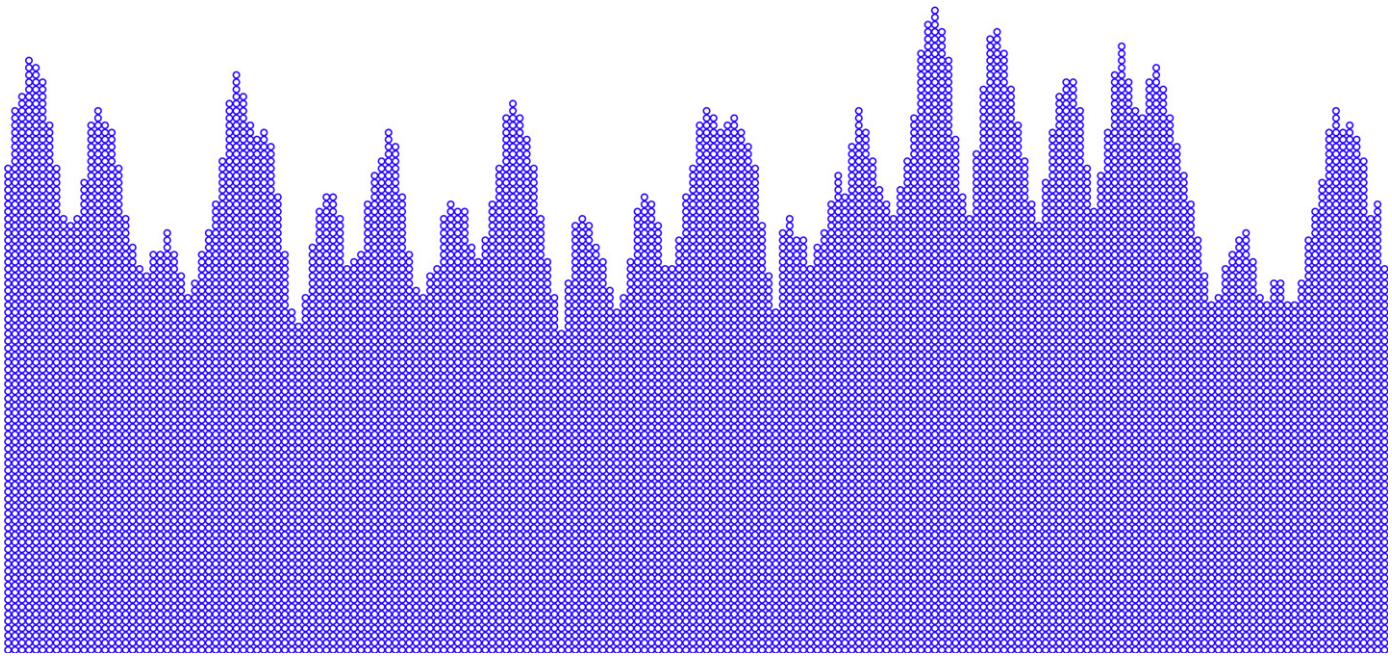

Fig. 12. A snapshot of the surface configuration at the end of the closed-loop simulation under the 40th-order output feedback controller: initial surface roughness is 0.5.

corresponding open-loop simulation value. A snapshot of the surface configuration at the end of the closed-loop simulation is shown in Fig. 12.

For output feedback control, $m = 20$ is also an appropriate dimension for the reduced-order system. Simulations under output feedback control with different dimensions of the reduced-order system are compared in Figs. 10 and 11 with different initial surface conditions similarly to the comparison of the state feedback controller in Section 5.2. In these figures, we can see that the output feedback controllers stabilize the expected surface roughness, but are not as effective as the state feedback controllers, especially when the dimension, m, is relatively small. In Fig. 10, the output feedback controller with $m = 1$ drives the expected surface roughness to a value which is higher than the one obtained under open-loop operation (see Fig. 7). In Fig. 10, we also observe that as the dimension (and thus the number of sensors) of the model used for controller design increases, the difference between the output feedback controllers and the state feedback controllers decreases. This is due to the decreased error of the estimated state as the number of measurements increases. We therefore conclude that $m=20$ is an appropriate value for the output feedback controller design.

6. Conclusions

In this work, we developed a method to estimate the parameters of the nonlinear stochastic KSE model and designed model-based state and output feedback controllers for a sputtering process, which includes two surface micro-processes and is simulated by a kMC model. Both parameter estimation and feedback control design begin with formulation of the stochastic KSE into a system of infinite stochastic ODEs by using modal decomposition. A finite-dimensional approximation is then obtained to capture the dominant mode contribution to the surface roughness profile. For parameter estimation purposes, a deterministic ODE model of the evolution of the state covariance is derived to eliminate the influence of fluctuations from the stochastic processes. Subsequently, a kMC simulator of the sputtering process is used to generate surface snapshots at different time instants during the process evolution to obtain the state and the state covariance of the stochastic ODE system. Finally, the model parameters of the nonlinear stochastic KSE are obtained using least-squares fitting and validated by comparing the KSE open-loop simulation result with the kMC simulation result. With respect to feedback controller design, two schemes are developed and applied to the sputtering process: state feedback control and output feedback control. Both control laws are demonstrated to effectively reduce the expected surface roughness compared to the open-loop operation.

Acknowledgment

Financial support from NSF, CBET-0652131, is gratefully acknowledged by Gangshi Hu and Panagiotis D. Christofides.

References

Akiyama, Y., Imaishi, N., Shin, Y.S., Jung, S.C., 2002. Macro- and micro-scale simulation of growth rate and composition in MOCVD of yttria-stabilized ziroconia. Journal of Crystal Growth 241, 352–362.

Armaou, A., Christofides, P.D., 2002. Dynamic optimization of dissipative PDE systems using nonlinear order reduction. Chemical Engineering Science 57, 5083–5114.

Armaou, A., Siettos, C.I., Kevrekidis, I.G., 2004. Time-steppers and 'coarse' control of distributed microscopic processes. International Journal of Robust and Nonlinear Control 14, 89–111.

Åström, K.J., 1970. Introduction to Stochastic Control Theory. Academic Press, New York.

Ballestad, A., Ruck, B.J., Schmid, J.H., Adamcyk, M., Nodwell, E., Nicoll, C., Tiedje, T., 2002. Surface morphology of gas during molecular beam epitaxy growth: comparison of experimental data with simulations based on continuum growth equations. Physical Review B 65, 205302.

Bohlin, T., Graebe, S.F., 1995. Issues in nonlinear stochastic grey-box identification. International Journal of Adaptive Control and Signal Processing 9, 465–490.

Choo, J.O., Adomaitis, R.A., Henn-Lecordier, L., Cai, Y., Rubloff, G.W., 2005. Development of a spatially controllable chemical vapor deposition reactor with combinatorial processing capabilities. Review of Scientific Instruments 76, 062217.

Christofides, P.D., Armaou, A., 2006. Control and optimization of multiscale process systems. Computers & Chemical Engineering 30, 1670–1686.

Christofides, P.D., Baker, J., 1999. Robust output feedback control of quasi-linear parabolic PDE systems. Systems & Control Letters 36, 307–316.

Christofides, P.D., Daoutidis, P., 1997. Finite-dimensional control of parabolic PDE systems using approximate inertial manifolds. Journal of Mathematical Analysis and Applications 216, 398–420.

Chua, A.L.S., Haselwandter, C.A., Baggio, C., Vvedensky, D.D., 2005. Langevin equations for fluctuating surfaces. Physical Review E 72, 051103.

Cuerno, R., Makse, H.A., Tomassone, S., Harrington, S.T., Stanley, H.E., 1995. Stochastic model for surface erosion via ion sputtering: dynamical evolution from ripple morphology to rough morphology. Physical Review Letters 75, 4464–4467.

Edwards, S.F., Wilkinson, D.R., 1982. The surface statistics of a granular aggregate. Proceedings of the Royal Society of London Series A—Mathematical Physical and Engineering Sciences 381, 17–31.

Fichthorn, K.A., Weinberg, W.H., 1991. Theoretical foundations of dynamical Monte Carlo simulations. Journal of Chemical Physics 95, 1090–1096.

Gallivan, M.A., Murray, R.M., 2004. Reduction and identification methods for markovian control systems, with application to thin film deposition. International Journal of Robust and Nonlinear Control 14, 113–132.

Gillespie, D.T., 1976. A general method for numerically simulating the stochastic time evolution of coupled chemical reactions. Journal of Computational Physics 22, 403–434.

Haselwandter, C., Vvedensky, D.D., 2002. Fluctuations in the lattice gas for Burgers' equation. Journal of Physics A: Mathematical and General 35, L579–L584.

Hotz, A., Skelton, R.E., 1987. Covariance control theory. International Journal of Control 46, 13–32.

Kan, H.C., Shah, S., Tadyyon-Eslami, T., Phaneuf, R.J., 2004. Transient evolution of surface roughness on patterned GaAs(0 0 1) during homoepitaxial growth. Physical Review Letters 92, 146101.

Kardar, M., Parisi, G., Zhang, Y.C., 1986. Dynamic scaling of growing interfaces. Physical Review Letters 56, 889–892.

Kloeden, P.E., Platen, E., 1995. Numerical Solutions of Stochastic Differential Equations. Springer, Heidelberg.

Kristensen, N.R., Madsen, H., Jorgensen, S.B., 2004. Parameter estimation in stochastic grey-box models. Automatica 40, 225–237.

Lauritsen, K.B., Cuerno, R., Makse, H.A., 1996. Noisy Kuramote–Sivashinsky equation for an erosion model. Physical Review E 54, 3577–3580.

Lee, Y.H., Kim, Y.S., Ju, B.K., Oh, M.H., 1999. Roughness of ZnS:Pr, Ce/Ta_2O_5 interface and its effects on electrical performance of alternating current thin-film electroluminescent devices. IEEE Transactions on Electron Devices 46, 892–896.

Lou, Y., Christofides, P.D., 2003a. Estimation and control of surface roughness in thin film growth using kinetic Monte-Carlo models. Chemical Engineering Science 58, 3115–3129.

Lou, Y., Christofides, P.D., 2003b. Feedback control of growth rate and surface roughness in thin film growth. A.I.Ch.E. Journal 49, 2099–2113.

Lou, Y., Christofides, P.D., 2004. Feedback control of surface roughness of GaAs(0 0 1) thin films using kinetic Monte-Carlo models. Computers & Chemical Engineering 29, 225–241.

Lou, Y., Christofides, P.D., 2005a. Feedback control of surface roughness in sputtering processes using the stochastic Kuramoto–Sivashinsky equation. Computers & Chemical Engineering 29, 741–759.

Lou, Y., Christofides, P.D., 2005b. Feedback control of surface roughness using stochastic PDEs. A.I.Ch.E. Journal 51, 345–352.

Lou, Y., Christofides, P.D., 2006. Nonlinear feedback control of surface roughness using a stochastic PDE: design and application to a sputtering process. Industrial & Engineering Chemistry Research 45, 7177–7189.

Makeev, M.A., Cuerno, R., Barabasi, A.L., 2002. Morphology of ion-sputtered surfaces. Nuclear Instruments and Methods in Physics Research B 197, 185–227.

Makov, G., Payne, M.C., 1995. Periodic boundary conditions in ab initio calculations. Physical Review B 51, 4014–4022.

Ni, D., Christofides, P.D., 2005a. Dynamics and control of thin film surface microstructure in a complex deposition process. Chemical Engineering Science 60, 1603–1617.

Ni, D., Christofides, P.D., 2005b. Multivariable predictive control of thin film deposition using a stochastic PDE model. Industrial & Engineering Chemistry Research 44, 2416–2427.

Ni, D., Lou, Y., Christofides, P.D., Sha, L., Lao, S., Chang, J.P., 2004. Real-time carbon content control for PECVD ZrO_2 thin-film growth. IEEE Transactions on Semiconductor Manufacturing 17, 221–230.

Reese, J.S., Raimondeau, S., Vlachos, D.G., 2001. Monte Carlo algorithms for complex surface reaction mechanisms: efficiency and accuracy. Journal of Computational Physics 173, 302–321.

Renaud, G., Lazzari, R., Revenant, C., Barbier, A., Noblet, M., Ulrich, O., Leroy, F., Jupille, J., Borensztein, Y., Henry, C.R., Deville, J.P., Scheurer, F., Mane-Mane, J., Fruchart, O., 2003. Real-time monitoring of growing nanoparticles. Science 300, 1416–1419.

Rusli, E., Drews, T.O., Ma, D.L., Alkire, R.C., Braatz, R.D., 2006. Robust nonlinear feedforward–feedback control of a coupled kinetic Monte Carlo-finite difference simulation. Journal of Process Control 16, 409–417.

Shitara, T., Vvedensky, D.D., Wilby, M.R., Zhang, J., Neave, J.H., Joyce, B.A., 1992. Step-density variations and reflection high-energy electron-diffraction intensity oscillations during epitaxial growth on vicinal GaAs(0 0 1). Physical Review B 46, 6815–6824.

Siegert, M., Plischke, M., 1994. Solid-on-solid models of molecular-beam epitaxy. Physical Review E 50, 917–931.

Siettos, C.I., Armaou, A., Makeev, A.G., Kevrekidis, I.G., 2003. Microscopic/stochastic timesteppers and "coarse" control: a kMC example. A.I.Ch.E. Journal 49, 1922–1926.

Varshney, A., Armaou, A., 2005. Multiscale optimization using hybrid PDE/kMC process systems with application to thin film growth. Chemical Engineering Science 60, 6780–6794.

Varshney, A., Armaou, A., 2006. Identification of macroscopic variables for low-order modeling of thin-film growth. Industrial & Engineering Chemistry Research 45, 8290–8298.

Villain, J., 1991. Continuum models of crystal growth from atomic beams with and without desorption. Journal de Physique I 1, 19–42.

Vlachos, D.G., 1997. Multiscale integration hybrid algorithms for homogeneous–heterogeneous reactors. A.I.Ch.E. Journal 43, 3031–3041.

Vlachos, D.G., Schmidt, L.D., Aris, R., 1993. Kinetics of faceting of crystals in growth, etching, and equilibrium. Physical Review B 47, 4896–4909.

Voigtländer, B., 2001. Fundamental processes in Si/Si and Ge/Si studied by scanning tunneling microscopy during growth. Surface Science Reports 43, 127–254.

Vvedensky, D.D., 2003. Edwards–Wilkinson equation from lattice transition rules. Physical Review E 67, 025102(R).

Vvedensky, D.D., Zangwill, A., Luse, C.N., Wilby, M.R., 1993. Stochastic equations of motion for epitaxial growth. Physical Review E 48, 852–862.

Zapien, J.A., Messier, R., Collin, R.W., 2001. Ultraviolet-extended real-time spectroscopic ellipsometry for characterization of phase evolution in BN thin films. Applied Physics Letters 78, 1982–1984.

Ziff, R.M., Gulari, E., Barshad, Y., 1986. Kinetic phase transitions in an irreversible surface-reaction model. Physical Review Letters 56, 2553–2556.